AD NUMBER

AD893795

LIMITATION CHANGES

TO:

Approved for public release; distribution is unlimited.

FROM:

Distribution authorized to U.S. Gov't. agencies only; Test and Evaluation; APR 1972. Other requests shall be referred to Arnold Engineering Development Center, Arnold AFB, TN 37389.

AUTHORITY

AFWAL ltr 3 Nov 1983

cy 2

RADIO TELEMETRY DEVELOPMENT FOR AEROBALLISTIC RANGE TESTS

R. H. Choate

ARO, Inc.

April 1972

VON KÁRMÁN GAS DYNAMICS FACILITY
ARNOLD ENGINEERING DEVELOPMENT CENTER
AIR FORCE SYSTEMS COMMAND
ARNOLD AIR FORCE STATION, TENNESSEE

NOTICES

When U. S. Government drawings specifications, or other data are used for any purpose other than a definitely related Government procurement operation, the Government thereby incurs no responsibility nor any obligation whatsoever, and the fact that the Government may have formulated, furnished, or in any way supplied the said drawings, specifications, or other data, is not to be regarded by implication or otherwise, or in any manner licensing the holder or any other person or corporation, or conveying any rights or permission to manufacture, use, or sell any patented invention that may in any way be related thereto.

Qualified users may obtain copies of this report from the Defense Documentation Center.

References to named commercial products in this report are not to be considered in any sense as an endorsement of the product by the United States Air Force or the Government.

RADIO TELEMETRY DEVELOPMENT FOR AEROBALLISTIC RANGE TESTS

R. H. Choate
ARO, Inc.

FOREWORD

The work reported herein was sponsored by Arnold Engineering Development Center (AEDC), Air Force Systems Command (AFSC), Arnold Air Force Station, Tennessee, under Program Element 64719F.

The results of the research and development reported herein were obtained by ARO, Inc. (a subsidiary of Sverdrup & Parcel and Associates, Inc.), contract operator of AEDC, AFSC, Arnold Air Force Station, Tennessee, under Contract F40600-72-C-0003. The research and development were conducted from July 1, 1970, to June 30, 1971, under ARO Project No. VG5104. The range test firings were conducted from April 8 to September 10, 1971, under ARO Projects No. VG0141 and VG0141, Revision A. The manuscript was submitted for publication on January 28, 1972.

Many of the items discussed in this report were not developed or manufactured to withstand the tests to which they were subjected, nor to operate as applied during this study. Any failure to meet the objectives of this study is no reflection on any of the commercial items discussed herein, nor on any manufacturer.

The author gratefully acknowledges the contributions to this report of many colleagues, particularly the following: R. P. Young, for work in circuit and model design; B. W. Gilley, for preparation of the data acquisition system; H. G. Love, for fabrication and encapsulation of the test models; M. K. Kingery, for assistance rendered during the test firing phase of the program; and J. C. Adams, Jr., for contributions to data reduction.

This technical report has been reviewed and is approved.

Marshall K. Kingery
Research and Development Division
Directorate of Technology

R. O. Dietz
Acting Director
Directorate of Technology

ABSTRACT

An aeroballistic range telemetry system, developed for heat-transfer measurements, was evaluated by means of static and dynamic tests and then subjected to actual range launchings. Heat-transfer information was telemetered from conical models in flight on two successive launches in the VKF 1000-ft Hyperballistic Range (G). The models, sharp, 10-deg (half-angle) cones of 2.0-in. base diameter, were in free flight near Mach 6 at free-stream pressures near 50 torr. Heat-transfer transducers were located on the conical surfaces at 69.4 percent of the distance from the nose to the base. Telemetered heat-transfer rates, in the vicinity of 25 Btu/ft^2-sec, were about 10 and 25 percent below theoretically predicted values on these two shots. Several possible reasons for disagreement between telemetered and theoretical data are identifiable.

CONTENTS

APPENDIXES

I. ILLUSTRATIONS

Figure

NOMENCLATURE

M_∞	Free-stream Mach number, dimensionless
p_∞	Free-stream pressure, units as shown
$\dot{q}$	Heat-transfer rate, Btu/ft^2-sec
$Re_{\infty, \ell}$	Reynolds number, based on free-stream conditions and model length, dimensionless
x/L	Model surface station, where x is a variable and L is model surface length, dimensionless
α	Pitch angle, deg
β	Yaw angle, deg
ϕ	Roll angle, deg
θ_c	Cone half-angle, deg

SECTION I
INTRODUCTION

A 1000-ft long, 10-ft diameter, variable-density range (Ref. 1), hereafter referred to as Range G, is included among the aerodynamic test units comprising the von Kármán Gas Dynamics Facility (VKF) of the Arnold Engineering Development Center. This range is well suited for such applications as the measurement of aerodynamic coefficients, static and dynamic stability testing, flow field diagnostics, or investigating any other parameter obtainable through external observables. The usefulness of such range test facilities would be greatly enhanced if aerodynamic data (i. e., pressures, heat-transfer rates) could be acquired from the surface of the free-flight model. Radio transmitters offer perhaps the best method at present for relaying such aerodynamic information from the models to remote recording stations. Satisfactory development of a reliable telemetry system for this purpose would represent a major breakthrough in hypervelocity range testing techniques.

A program was initiated to demonstrate a telemetry capability to provide aerodynamic measurements from free-flight models. The test model selected was a sharp, 10-deg (half-angle) cone. The goal of the program was to acquire surface heat-transfer rate data via telemetry at a flight velocity near 7000 ft/sec in Range G.

A simple, Colpitts oscillator was selected as the basic telemetry transmitter because similar transmitters (but without transducers) had operated satisfactorily after surviving peak launch accelerations in excess of 100, 000 g in another VKF range facility (Ref. 2). In a preliminary evaluation of this same type of transmitter in Range G, at peak launch accelerations near 80, 000 g and velocities near 10, 000 ft/sec, it was found that telemeter performance was generally poor. However, further launches at different range pressures led to the conclusion that much of this poor performance in Range G could be attributed to interactions between the electromagnetic radiation from the transmitter and the overdense plasma in the flow field of the blunt test model used at these velocities. The use of a sharp conical model would reduce ionization effects by orders of magnitude because the velocity would be lower, and a peak launch acceleration of only 30, 000 g would be needed. Thus, no severe difficulties were anticipated in successful completion of the proposed Range G program.

The suitability of the telemetry transmitter, model, and sabot for the proposed application was to be verified by means of static compression tests and dynamic impulse tests before commitment to a

Range G launch schedule. The credibility of the range results was to be assessed by comparing the telemetered data with wind tunnel or theoretical data.

SECTION II
MODELS AND SABOTS

2.1 IMPULSE TEST MODEL

A right-circular cylinder with a removable, hemispherical, nose cap (Fig. 1, Appendix I) was used during the impulse tests to adapt the telemetry test packages to the 2.5-in. bore of the launcher. The impulse model was made of plastic to allow radio transmission through the model wall. Silicone rubber was cast into the tapered section (Fig. 1) to furnish protection for the telemetry package upon deceleration and impact. No sabot was required, as the projectile diameter was the same as the launcher bore.

2.2 RANGE TEST MODELS AND SABOTS

A sharp, 10-deg, half-angle cone model with a 2-in. base diameter was selected as the test model for the Range G launches. Two different types were designed; one with a plastic afterbody, and the other with an aluminum afterbody. Drawings of these models are shown in Fig. 2. The transmitter in each model is packaged within an epoxy-fiber glass cup for reinforcement. The cup is mechanically isolated from the model structure by an air gap, as can be seen in Fig. 2, and thus, should be protected from inertial loading by the model during launch.

A model with a plastic afterbody (Fig. 2a) was designed for use during the initial tests at 7000 ft/sec. Approximate weight of this model was 0.385 lb (175 grams). Calculations indicated that this model could withstand peak launch accelerations near 42,000 g, whereas the peak acceleration expected for the 7000 ft/sec launches was near 30,000 g.

The metal model (Fig. 2b) was designed primarily for possible follow-up tests at higher velocities. An analysis indicated that this model should withstand 12,000 ft/sec launches. It was also to be used in the laboratory to perfect techniques for transmitting from all-metal models. Assembled weight of this model was 0.495 lb (225 grams).

The models were adapted to the 2.5-in. -diam launch tube bore by sabots which were stripped away by aerodynamic forces when the models exited the bore. Generally, a four-piece sabot was used, such as is shown in Fig. 3 with a typical model. A five-piece sabot was also available. This was similar to the four-piece sabot shown but had an additional, bore-sized plug behind the model to act as a gas check. The mating surfaces of the sabots were saw-toothed, as shown in Fig. 3; this was done to decrease muzzle gas leakage through the sabot to the model during launch.

SECTION III
RANGE G

An overall view of Range G is shown in Fig. 4 (Ref. 1). This range is equipped with a two-stage, powder-hydrogen launcher. Launch tube length is near 42 ft, with a bore of 2.5 in. The range test section is basically a 10-ft diam, 1000-ft long, evacuable steel tube. The initial 85 ft of the range is a blast chamber to absorb the expanding muzzle gases. Also, sabots are separated from the model here.

The two-stage launcher imparts a quite different acceleration-time characteristic to the test model from that of the single-stage launcher used in prior telemetry tests. In the single-stage launcher of Ref. 2, for instance, cold gas (generally, helium) was introduced into a chamber until a diaphragm ruptured, instantaneously applying the peak pressure to the test model in the barrel; thus, the acceleration decayed rapidly from its initial peak value. Later, the single-stage launcher of Ref. 2 used a powder driver to provide higher velocities. Here, the propellant gas contained powder combustion products and combustion-heated precharge gas (if used). In the two-stage launcher, ignition of the powder charge drives a piston down a pump tube. Ahead of the piston is an uncontaminated propellant gas (hydrogen in the Range G case). Because there are many parameters which may be adjusted to influence the performance of a two-stage launcher, many different model acceleration-time histories are possible for a given muzzle velocity. The two-stage launch generally can be made "softer" than the single-stage launch. (That is, for a given velocity, the peak acceleration during a two-stage launching can be made lower than that during a single-stage launching.) The use of the two-stage launcher for the present tests presupposed that the telemetry techniques developed in single-stage launchers were compatible with the existing two-stage launch cycle.

The primary range instrumentation systems used in the telemetry experiments were the dual-axis, spark shadowgraph stations, as described in Ref. 3, and the front-light laser photographic systems, described in Ref. 4. These two systems provided the necessary information to obtain model integrity, attitude, and velocity, as well as permitting an examination of model surface condition in flight.

SECTION IV
TELEMETRY SYSTEM

4.1 TRANSMITTING SYSTEM

A Colpitts oscillator configuration was chosen as the basic transmitter circuit. This type oscillator (as shown in Fig. 5) can be frequency modulated by varying the value of the emitter resistor, R1; thus, a variable resistance transducer may be used. Operating frequency was nominally 150 MHz with the component values shown. The value of R_{bias} (nominally 68 k Ω) was selected to result in a nominal current drain from the supply of 1.2 ma. The power supply for this and all following transmitters was a series-connected string of four each RM400 or RM400R mercury cells, for a supply voltage of nominally 5.4 volts.

4.1.1 Thin-Film Transmitter

The passive components (excluding the coil) shown in the circuit diagram in Fig. 5 were deposited on a sapphire substrate using in-house, thin-film evaporation techniques. The sapphire substrates used were 420 by 320 by 30 mils, with a 250 angstrom surface finish on flats. Nichrome was used for resistors, copper for interconnecting conductors, aluminum for capacitor plates, and silicon monoxide for the capacitor dielectric. An NS 9739 transistor was used with thin-film transmitters. This transistor is similar, electrically, to the 2N918 in Fig. 5, but packaged in chip form and having 5-mil-diam gold leads.

4.1.2 Cordwood Transmitter

The circuit diagram in Fig. 5 was also used for constructing transmitters with cordwood-type components. All of the components shown in Fig. 5 are commercially available, with the exception of the heat-rate transducer ($\dot{q}$ gage), which was fabricated in-house. The 2N918 transistor can was opened on a lathe, then potted internally with (warmed, outgassed) Armstrong C-7®, 8 phr Activator A®. The other

components were used as purchased. The resistors were 1/8- or 1/10-watt carbon resistors; the capacitors were NPO glass-dielectric, glass-case types.

4.1.3 Cordwood-VVC Transmitter

A cordwood-component transmitter which used a voltage-variable capacitor (VVC) to permit isolation of the transducer from the RF portion of the circuit was also constructed, using the circuit diagram shown in Fig. 6. Bias for the VVC (a back-biased diode) was provided by a resistive divider, with the transducer forming one of the legs. As the transducer was heated, its resistance increased. This lowered the voltage across the VVC, increasing its capacitance, thereby lowering transmitter operating frequency. The 150-pF capacitor and the 56-k ohm resistor provided dc and RF isolation of the gage from the transmitter. Current drain for the circuit shown in Fig. 6 was adjusted to nominally 2.1 ma by varying the R_{bias} value.

An MSI Electronics type G 610 was selected as the VVC to be used, for three reasons. First, its capacitance of 10 pF at 4 v was compatible with the VKF circuit. Second, the modulation sensitivity (transmitter deviation/unit gage resistance change, kHz/ohm) using this VVC would equal or exceed that of the previous modulation technique. Third, the void-free construction of this device greatly enhanced the possibility of satisfactory operation after gun launch.

4.1.4 FM/FM Transmitter

An FM/FM transmitter was also developed, as a backup system in case difficulties were encountered with VVC modulation, and to establish a basis for multichannel gun-range telemetry operation. Cordwood components were used throughout.

In this FM/FM system, the same type transducer as was used in the Colpitts-VVC transmitter was now used to frequency modulate a low-frequency (~24kHz), subcarrier oscillator. Simultaneously, the subcarrier oscillator frequency modulated the 88 MHz VHF transmitter. Multichannel data acquisition with an FM/FM system would require only an additional subcarrier oscillator for each data channel. (The above direct modulation systems require a complete, separate, transmitter and receiver for each channel.) The details of this FM/FM system are summarized in Appendix III.

4.2 TRANSDUCER ($\dot{q}$ Gage)

The $\dot{q}$ gage designed for the gun-range tests is shown in Fig. 7. This slug calorimeter design used a variable-resistance, semiconductor, temperature sensing element (Temp Sensor®) bonded to the back of a 20-mil disk of 2024-T4 aluminum. Nominal room-temperature resistance was 1000 ohms. The body shell of the transducer was cast from Emerson and Cuming Stycast 1090® epoxy resin, and the disk was bonded to it with epoxy. The gage was contoured to adapt to the curvature of the cone model wall. This type gage is referred to as Type A in the discussion which follows.

Bench tests (tension, compression, and shear) indicated that the Type A gage could withstand static loadings corresponding to launch accelerations near 250,000 g. However, two failures out of three launchings in Range G were later identified as gage failures (open circuit) during preliminary launchings at peak accelerations near 30,000 g; therefore, the Type A gage was further ruggedized. Four pins were secured to the calorimeter disk. These pins extended down into the epoxy body shell, which was filled completely, leaving no air void of the kind shown in Fig. 7. In addition, the gage was enclosed in a 302 stainless steel ring of 5/16-in. OD to decrease inertial loading of the gage by the model structure during acceleration. This type gage will be referred to as Type B. Bench tests indicated that the gage heat losses resulting from the addition of an epoxy backing to the calorimeter disk should not be significant in the intended application.

4.3 ENCAPSULATION

The same potting mixtures and procedures were used throughout for encapsulating the telemetry units and individual components for static compression tests, impulse tests, and range tests. A filler, 20 percent by weight of 1/32-in. milled fiber glass, was added to the base epoxy resin used, Armstrong C-7, to increase its impact strength. Eight percent by weight (of the unfilled base epoxy) of Activator A was then added. The potting mixture was heated (~120°F) to improve flow characteristics, then vacuum outgassed to remove air bubbles before pouring. A vibrator table was generally used to improve further the flow characteristics of the potting material around the components. Epoxy cure was in a pressurized chamber at 50 to 75 psig and room temperature.

The static compression and impulse test slugs were right-circular cylinders of the above potting materials, with the components or circuits

to be tested embedded inside. These slugs were 1.125-in. in diameter by 1.5-in. long, with the ends machined flat. These dimensions are sufficient to accommodate the entire telemetry transmission system, including transmitter circuitry, gage, and batteries.

The range test circuits were encapsulated in small fiber glass cups, such as the one shown in Fig. 2. These cups have inside dimensions of 0.7-in. in diameter by 0.6 in. deep. Neither the batteries nor the gage are contained in this cup, only the transmitter circuitry. The batteries and gage are located as shown in Fig. 2a; thus, three wires not supported by potting material were required (shown by the dotted lines in Fig. 2a) to connect the gage, circuitry, and batteries. Figure 8 is a photograph of the on-board telemetry components prior to the encapsulation process, showing the relative sizes of the model, fiber glass cup, transmitter circuitry, gage, and batteries.

4.4 RECEPTION AND RECORDING SYSTEM

4.4.1 Antenna System

In developing the antenna system for telemetry reception, the 10-ft-diam, 1000-ft-long range tank was considered as a crude waveguide. In previous work (Ref. 2), this approach had greatly simplified the antenna system needed in a 6-ft-diam, 100-ft-long range. In that case, only one (free-space) quarter-wavelength stub antenna was needed for reception throughout flight. However, the Range G tank was found to be quite lossy when evaluated as a 150-MHz waveguide. Attenuation levels were measured and found to be 10 to 15 dB/100 ft. To provide adequate reception, several stub antennas were spaced along the range (Fig. 9) and interconnected by coaxial cable (3 dB/100-ft attenuation).

At the nominal telemeter operating frequency of 150 MHz, propagation would have been possible in any one of six different modes (TE_{11}, TM_{01}, TE_{21}, TM_{11}, TE_{01}, TE_{31}). The radial stubs protruding from the range walls provided adequate reception, making it likely that the energy was being propagated in one of the TE modes. Attempts to determine the mode or modes of propagation by measuring guide wavelengths[1] were inconclusive, presumably because of multiple reflections from hardware inside the range.

A large bulkhead across the range tank near shadowgraph station 14 effectively divided the range into two separate waveguides. This,

[1]Note that the "waveguide" is short circuited at both ends; hence, standing waves will occur.

together with the multiple stub requirement, gave rise to a novel re-radiation and coupling technique, as shown in Fig. 9. The two stubs nearest shadowgraph station 23 are the main pickup stubs, which should furnish telemetry information throughout model flight. Telemetry signals uprange of the bulkhead cannot propagate through it. However, they are collected by secondary pickup stubs, routed past the bulkhead by coaxial cable, amplified, and reradiated by other secondary stubs to the main pickup stubs, using the waveguide as a coupling medium.

A long wire antenna is also available uprange of the bulkhead. During comparative tests of the long wire and stub antenna systems, it was determined that the stub antenna system was superior and, further, that installation of a long wire enhanced pickup from the stub system even more. So, the long wire has been retained – as a separate uprange antenna system, and as an aid to the stub antenna system.

Transistorized line-drive amplifiers, fabricated in-house, were used to amplify the signal as it was routed past the bulkhead and to overcome losses in the cables leading to the control room receivers. These amplifiers have a nominal gain of 25 dB over a bandwidth of 100 to 200 MHz.

4.4.2 Receivers and Recording Equipment

A six-channel, mobile, receiving and recording system was assembled for the tests. In addition to the telemetry receivers, this system contained an RF distribution amplifier (multicoupler), data signal conditioning amplifiers, and a recording oscillograph.

The function performed during a typical range test by each of the six receivers, a tabulation of receiver characteristics, and the antennas used by each, are summarized in Table I (Appendix II). A brief explanation of the significance of receiver characteristics in direct frequency modulation, as employed in the present telemetry work, is in order at this point.

When direct modulation techniques are employed, the receivers used for data acquisition should have high sensitivities and wide bandwidths, with linear discriminator characteristics. High sensitivity is desirable because the FM discriminator output voltage (the amplitude of which represents transmitter frequency deviation) is a function of the incoming RF signal level, when the incoming level is below a certain value. Thus, the higher the receiver sensitivity, the less the incoming signal level required for satisfactory data acquisition. This is covered in detail in Ref. 5, where techniques are described to define this

minimum level. A wide bandwidth is desirable because the transmitter often shifts operating frequency during gun launch. Thus, the wider the bandwidth, the more likely the possibility of data recovery. A linear discriminator characteristic is desirable for accuracy in data reduction.

Of the six receivers used during these tests, only two fulfilled the desired characteristics mentioned above. These two were solid-state units with 3.3-MHz bandwidths, linear discriminator characteristics, and requiring about 6 microvolts input for satisfactory operation. Another solid-state receiver available had a (linear) bandwidth of 1.0 MHz, and required about 4 microvolts input. The remaining receivers were older, tube-type units, which typically required 60 microvolts input. Though their bandwidths were nominally 1.2 MHz, the discriminator characteristics were linear only over about 500 kHz.

A frequency deviation of the transmitter caused by a gage resistance change results in a change in the (direct-coupled) FM discriminator output voltage of the receiver. Thus, this voltage is an analog signal relatable to the transducer's input. This signal is conditioned by a dc amplifier circuit to drive either a galvanometer in the recording oscillograph, or an FM channel of a magnetic tape system. A simplified single-channel diagram, representative of all six channels, is shown in Fig. 10. As seen here, a dc signal from the receiver relatable to incoming RF level is also recorded on the oscillograph, for reasons mentioned previously.

SECTION V
CALIBRATION

An air-acetylene torch, similar to the type described in Ref. 6, was used for telemetry system calibration. The heat-transfer rate from the torch had been determined using a thermocouple heat-transfer gage (Ref. 7) as a calibration standard. Figure 11 shows the calibration apparatus and a gage-equipped model to be calibrated. In operation, the torch rotates so that the flame impinges on the gage for a preset time interval.

A linear calibration constant of the form $K = \frac{Btu/ft^2\text{-}sec}{kHz/sec}$ was obtained for each of the on-board telemetry systems during calibration. Linear constants could be assigned because, under the calibration conditions selected,

1. Calorimeter disk temperature rise versus time was linear, for a constant heat input (Ref. 7);
2. The temperature rise at the back surface of the calorimeter disk (where the sensing element was affixed) was approximately the same as the average temperature rise of the entire disk (Ref. 7);
3. The resistance change of the sensing element was linear with respect to temperature;
4. The frequency deviation of the telemetry transmitter was linear with respect to gage resistance changes; and
5. The receiver FM discriminator output voltage was linear with respect to transmitter frequency deviation.

SECTION VI
BENCH TESTS AND RESULTS

Before committing a telemetry-equipped model to a launch schedule, the telemetry system was subjected to various bench tests to evaluate its electrical performance. Static compression tests and dynamic impulse tests were then performed, to determine the mechanical soundness of the selected system.

During subsequent range tests, it became obvious that, of the three direct modulations systems described previously, only the Colpitts-VVC system appeared capable of furnishing satisfactory, inflight data without further development. (The FM/FM system was not range tested.) For this reason, only the tests and results which pertain to evaluation of the VVC telemetry circuitry and gage are reported.

6.1 ELECTRICAL TESTS

The electrical performance of the VVC-modulated transmitter (Fig. 6) was found satisfactory for making the intended gun-range measurements. The modulation sensitivity was from three to five times greater than that of the earlier transmitters depicted schematically in Fig. 5. Moreover, the modulation sensitivity was not affected by gage lead length, and the transmitter operating frequency was not affected by proximity of the gage to metallic or non-metallic objects. Such was not the case with the earlier transmitters.

Two disadvantages arose from the use of VVC modulators. First, the VVC circuit required a greater number of components, increasing the component packaging density in the space available aboard the model. Second, the transmitter operating frequency was more voltage sensitive than on previous transmitters because a changing supply voltage caused the VVC capacitance to change. The supply voltage sensitivities of the VVC transmitter and other transmitters are shown in Fig. 12. (The FET-Hartley characteristics shown in Fig. 12 are of the FM/FM transmitter described in Appendix III.) The voltage sensitivity of the VVC transmitter was not considered a serious problem because evidence of fluctuating battery voltage had not appeared in past gun-range tests.

The effect of individual component failure on transmitter operation was investigated. Each capacitor in the Colpitts-VVC transmitter was disconnected, and the effect was noted. These results are presented in Table II. (Figure 6 is reproduced for reference.) Note that if the 150-pF bypass capacitor between base and B- opens, the operating frequency may change anywhere between ±2 MHz. The operating frequency in this case was found to be strongly dependent on the orientation and length of the battery leads inside the cone model. Of the resistors, only the gage was disconnected to simulate failure; the operating frequency dropped approximately 8.5 MHz.

6.2 STATIC COMPRESSION TESTS

Static compression tests were conducted to determine the mechanical ruggedness of the VVC transmitters, using the apparatus shown in Fig. 13. The load applied by the hydraulic press was monitored by a 20,000-lb load cell and displayed on the X axis of the X-Y plotter. Any shift in transmitter frequency resulted in a proportional change in receiver discriminator output voltage and was displayed on the Y axis.

The VVC transmitters for the static compression tests were constructed using the same component mounting fixture which was later used for construction of the gun-range transmitters. The batteries and gage were external to the static compression test slug and the potting procedures and techniques outlined in Section 4.2 were followed.

Maximum load applied during these static compression tests was 10,000 lb, whereas the maximum compressive load calculated for the transmitter package during a 30,000 g launch was about 600 lb. The value of 10,000 lb, therefore, provided compressive loads far in excess of the expected loading. During the static compression tests,

increasing loads were applied to the test specimens in 2000-lb increments. At each condition, the load was gradually increased to its maximum value, then removed completely before commencing the next loading.

The load-frequency characteristics of two VVC-equipped test specimens are shown in Fig. 14. As seen here, the receiver was not retuned following each load removal, so that the load-induced frequency shift would accumulate. It is obvious from Fig. 14 that one or more components in DM-2 were behaving erratically under load, as indicated by the frequency "jumps." The data resulting from these tests are presented in Table III, as are the test results of non-VVC transmitters for comparison. As seen here, there are no significant differences between the two sets of results, either in permanent frequency shift remaining after 10,000-lb load removal, or in frequency jumps during the tests. Each of the VVC-modulated transmitters had been calibrated to determine the frequency deviation versus gage resistance change (modulation sensitivity) prior to the test. There were no significant differences in this parameter after the static compression tests.

The jumps in transmitter operating frequency noted in the Comments column of Table III, and shown in Fig. 14, merited further investigation. Transistors and glass capacitors were tested first because they were suspected of producing this erratic behavior. Static compression tests on individual transistors produced no abnormal results. Permanent frequency shifts never exceeded 20 kHz after removal of 10,000-lb loads, and no frequency jumps were noted. Also satisfactory were 10,000-lb load tests on glass capacitors (10 pF). However, a large frequency jump, similar to those encountered during tests of complete transmitters, was recorded for one of the three capacitors tested when it was loaded further to 12,000 lb. (It should be pointed out that failures may occur at lower loads when testing complete packages – or during range tests – if increased component packaging densities inside the specimen result in stress concentrations.)

Further static compression tests indicated that capacitors of the larger values were particularly susceptible to failure under load. The 220-pF glass capacitor in one test specimen, for instance, failed (opened) during cure of the epoxy test specimen and before any external load had been applied. In two other test specimens, 220-pF capacitors failed at low applied loads. Because 150-pF capacitors appeared less failure prone than 220-pF capacitors during further testing, they were selected for use as bypass capacitors in the telemetry circuits. Even though they survived static loadings far in excess of the expected compressive loads during a gun launch, it was recognized at this time that they were weak links, in that they would be the first to fail.

Two carbon resistors and two RM400 mercury cells were also tested. Permanent resistance change on both resistors was less than one percent after removal of a 12,000-lb load. No effect at all was seen in output voltage or current on the two battery specimens tested to 12,000 lb.

6.3 OTHER STATIC TESTS

6.3.1 Batteries

The RM400-type mercury batteries used as the transmitter power supply were studied to determine possible modes of failure in high acceleration environments. The RM400-type cell has a unique anode configuration which gives rise to an open-circuit failure possibility. The anode is a hard pellet, rather than the jelled amalgam anode prevalent in other type cells, and thus could move away from the metal case during high acceleration launches, breaking electrical contact. A simple experiment showed that the open-circuit failure mode was not likely to occur in this application. The RM400-type cell was found to operate satisfactorily at the desired current drain (2 ma) for at least nine seconds after the cell had been cut open and the anode pellet removed. Failures also have been observed in the past as a result of internal shorting by the free mercury liberated during storage or normal discharge. This failure mode, also noted by other researchers (Ref. 8), is discussed briefly below.

The RM400R was used during the initial gun-range experiments; however, concurrent comparison tests of the RM400 and the RM400R, relating to battery failure by free mercury shorting, indicated that the RM400 should be superior for the AEDC gun-range application. This results because the RM400's depolarizer has the capability to disperse the mercury liberated; the depolarizer in an RM400R does not. This capability is shown in Fig. 15, which is a photograph showing free mercury accumulation in both type cells at different percent usages (based on mah rating). Only the depolarizer, the bottom case, and the mercury liberated are visible in Fig. 15; the rest of the components have been removed. During these bench tests, RM400R cells began failing at 21 percent of rated mah capacity because of free mercury shorting. None of the RM400's failed for this reason.

It has been noted during these experiments that internal cell degeneration (hence, free mercury buildup) on the shelf first takes the form of deterioration of the anode pellet. Because of the pellet anode, the RM400-type cells exhibit an unusual characteristic. When switched

across a short-circuit load (~1 ohm), the cell normally will surge a short-circuit current from 175 to 250 ma for a period of one-half to three seconds, after which time the current drops abruptly to a low value (passivates). However, this passivation capability ceases as soon as the pellet anode starts to deteriorate; thus, a simple short-circuit test provides an indication of the internal condition of the cell's anode. All cells are short-circuit tested before gun-range use; those which do not passivate in the prescribed manner are rejected.

6.3.2 $\dot{q}$ Gage

Several static tests were performed on the Type A gage (Fig. 7) in an attempt to evaluate its suitableness for gun-range work. The epoxy joint between the aluminum calorimeter disk and the body shell was statically tested in compression, tension, and shear because of its suspected vulnerability during a gun launch. The results indicated that the Type A gage was satisfactory for launch accelerations in excess of 250,000 g, giving a safety factor of about eight for the proposed tests.

Further tests and calculations were performed on the Type A gage in regard to the unsupported lead wires from the sensing element (Fig. 7), and the possibility of the gage accidentally being exposed to gun chamber pressures up to 10,000 psi. Test results showed that the lead wires should be satisfactory for conditions in excess of 250,000 g. Applying 10,000 psi to the calorimeter disk caused a maximum resistance change of no more than two percent, with no permanent damage observed.

Despite the apparent suitability of the Type A gage, it subsequently failed (opened) during two out of three gun launches. The gage was modified, and the Type B gage resulted, as described previously; however, no further static tests were performed, because of their apparent lack of effectiveness in simulating the real thing - the gun launch. Instead, the Type B gages were evaluated in the impulse test facility using telemetry transmitters and with the gages installed in cone models identical to those which would be used in range tests.

6.4 IMPULSE TESTS

Impulse tests were conducted using the apparatus depicted in Fig. 16. As seen here, the impulse tester is essentially a powder-hydrogen launcher equipped with an extremely short (14.5-in.) barrel. Use of a short barrel allows a high peak acceleration to be applied to a test specimen without imparting a launch velocity so high that deceleration and recovery of the specimen become impractical.

Typically, diaphragms (Fig. 16) with burst pressures of 10,000 psi were used for these tests. Thus, the peak accelerations, which were applied instantaneously when the diaphragms opened, were in the vicinity of 50,000 g for the 1-lb models tested, with launch velocities near 1000 ft/sec resulting in the evacuated (10 torr) test chamber. A rag-filled barrel (Fig. 16) was used to stop the test specimens. Satisfactory reception was not obtained while the telemetry-equipped specimens traversed the 12-ft-long connecting tube shown in Fig. 16; data acquisition was limited to the time the specimen was in flight within the test chamber.

6.4.1 Thin-Film Transmitters

Four of the thin-film transmitters had been installed in gage-equipped cone models and outfitted with sabots for impulse testing. Because the impulse tester was not completed at the time and because Range G was available, it was decided to conduct the impulse tests in Range G. These results are described in Section VII.

6.4.2 Cordwood Transmitters

No impulse tests were performed on the (non-VVC) cordwood transmitters.

6.4.3 Cordwood-VVC Transmitters

Three of the cordwood-VVC transmitters equipped with Type A gages were impulse tested. These circuits were encapsulated in right-circular cylinders and inserted into the impulse test model shown in Fig. 1. Since similar transmitters have operated after surviving peak launch accelerations of over 100,000 g (Ref. 2), failure of the transmitters to operate properly in the impulse facility was to be attributed to failure of either the VVC or the gage. To detect such failure, receivers were tuned to the frequencies to which the transmitter would shift if either the VVC or the gage failed. The normal operating frequency was monitored with a third receiver.

During the first of these impulse tests, the transmitter frequency during flight was only 20 kHz different from the pre-launch frequency. The plastic test model (which was hoped to be recoverable after firing into the rag-filled barrel) was badly damaged. The transmitter package was recovered, and it was found that the battery leads had been disconnected during impact. The transmitter operated normally when the leads were reconnected. A means had been provided during assembly to evaluate the modulation sensitivity of the transmitter circuit by

means of a decade resistance box. Modulation sensitivity was 1.24 kHz/ohm before, and 1.18 kHz/ohm after, the high acceleration launch and impact. The gage resistance still varied with heat input, indicating no major damage.

During the second test, both the plastic model and the transmitter package broke up on impact. Transmitter frequency in flight was about 100 kHz different from its value 1.5 hours before launch.

The third firing in the impulse tester resulted in an in-flight signal with a frequency within 20 kHz of the pre-launch value. Both the plastic test model and the gage were destroyed on impact. The remains of the telemetry package were recovered; recalibration using a resistance box showed the modulation sensitivity to be essentially unchanged from pre-launch value.

Even though the performances of both the VVC and the gage were satisfactory during these tests, such was not the case in two out of three subsequent Range G shots during which gage failures occurred. Since the Type A gage used in the impulse tests was potted into the front of the cylindrical test model, it was reasoned that there was little mechanical load transferred to the gage during the impulse tests. From this, it was surmised that loading of the gage by the cone model structure was responsible for the gage failure during Range G tests; therefore, the gage was ruggedized, as described previously, and no further impulse tests were conducted using cylindrical test specimens.

6.4.4 Type B Gages

Two of the ruggedized, Type B gages were installed in transmitter-equipped cone models. These models, identical in every respect to those which would be launched in Range G, were sabot equipped and launched in the impulse tester at nominally 40,000 g accelerations. One of the cone models was fitted with a cordwood-VVC transmitter; the other contained an FM/FM transmitter of the type described in Appendix III.

Operating frequency in flight was 160 kHz different from pre-launch frequency when the VVC-equipped model was launched in the impulse facility. No indication of gage heating was seen, and the model was totally destroyed upon impact. The fact that it operated within the receiver passband indicated that the Type B gage had survived the launch. The observed frequency shift of 160 kHz could be launch induced, but in this case could also be a detuning of the transmitter, caused by an unseparated sabot at this low free-stream pressure (10 torr).

Photographic coverage was not available in the impulse test chamber to verify this.

The model containing the FM/FM transmitter and a Type B gage was then launched. Subcarrier oscillator (SCO) frequency prior to launch was 26.33 kHz. During flight, the SCO frequency was 25.60 kHz. (The SCO frequency would have shifted to 10.0 kHz, had the gage open circuited.) Only the fiber glass cup and its contents (the telemetry electronics) were recovered. When the recovered telemeter was energized from a laboratory power supply (using a fixed 1000-ohm resistor in place of the destroyed gage), operation was satisfactory.

SECTION VII
RANGE TESTS AND RESULTS

In all, 12 launchings were made in Range G for various purposes using three different types of transmitters. All 12 launchings are briefly summarized in Table IV. Specific details are discussed in this section.

7.1 THIN-FILM TRANSMITTERS

The first four range launchings were thin-film transmitter impulse tests. Three of the thin-film transmitters were equipped with Type A gages; however, the gage on one of the models was recessed, and covered with epoxy so that gage heating would not occur. On the fourth, a fixed carbon resistor replaced the gage.

The first launching was of a transmitter with a normally installed gage. During range flight, the data trace showed a large (-500 kHz) frequency offset with a slight negative slope throughout flight. From a data interpretation viewpoint, the negative slope would indicate a heat transfer from the model to the surroundings. Such an occurrence is considered highly improbable. The large offset, or frequency shift, most likely resulted from either a circuit malfunction, or from an excessively high heat rate during launch. (A high heat rate would produce a saturation condition causing an essentially constant frequency deviation of the transmitter, a peculiarity of this particular thin-film design.) The data trace showed slight fluctuations which appeared to be relatable to the frequency of model motion in flight, indicating that the gage was possibly responding to a varying heat rate.

The second launching was of the transmitter with the gage recessed and covered with epoxy. No gage heating and, thus, no heat-transfer data were expected. The in-flight data trace showed a constant frequency shift of +600 kHz, with no fluctuations. The lack of fluctuation was felt to verify that the gage was modulating the transmitter on the previous shot. The frequency shift of 600 kHz indicated either a circuit malfunction, or possibly, a permanent deformation of the gage caused by excessive loading during launch.

A transmitter equipped with a normally installed gage did not operate in flight during the third launching. This could have been caused by a circuit malfunction, or by gage failure, since, as seen in Fig. 5, if the transducer opens, the transmitter shuts down. A five-piece sabot was used for this third launch in an attempt to provide better protection to the model (and gage, in particular) from hot driver gases during launch. This was done as a result of the indication of a possible high heat rate during the first launch.

During the fourth launch, in which the gage had been replaced with a fixed resistor, no output was recorded in flight. It was concluded at this time that the circuitry was malfunctioning, and the use of thin-film transmitters was discontinued.

7.2 CORDWOOD TRANSMITTERS

Cordwood circuitry was used for shots 2662 and 2663, using transmitters of the type shown in Fig. 5 and Type A gages. During shot 2662, the model failed in the barrel during launch. It was later concluded that the cause of failure was separation of the five-piece sabot during pump-down of the launch tube, allowing the model to slide out of the sabot.

A metal model was launched for shot 2663 and was so far off course that it impacted a shield about midrange. The poor launch was attributed to the five-piece sabot used. In view of this, and the possible sabot separation in the barrel on the previous shot, use of a five-piece sabot was discontinued. The transmitter in the metal model operated throughout flight with a frequency shift of approximately +260 kHz. Again, the data record showed fluctuations at about the same frequency as the measured (from shadowgraph data) model motion, indicating some modulation of the transmitter. The data record also indicated a slight, negative, heat-transfer rate. This was essentially the same data result as observed on the first thin-film launch. It was felt at this time that the lack of data so far had resulted from peculiarities caused by the gage forming part of the transmitter's RF circuit; therefore, a change was made to indirect, cordwood-VVC modulation.

7.3 CORDWOOD-VVC TRANSMITTERS

Three cordwood transmitters using VVC modulation and Type A gages were then launched -- shots 2810, 2811, and 2812. During shot 2810, there was a large frequency shift (-600 kHz), indicating either excessive gage heating or circuit malfunction. The transmitter ceased operating about 1/3 of the way down the range, indicating possible in-flight gage failure. This possibility could not be verified because the model had passed the section of range tank where reception of the frequency corresponding to gage open-circuit was possible (see Table I and Fig. 9). During shots 2811 and 2812, the transmitters emitted strong signals, with no frequency changes during flight, but at frequencies corresponding to open-circuit gage conditions, approximately 8.5 MHz below normal operating frequencies. Thus, gage failures were positively identified. In addition, the model had come apart during launch on shot 2812, failing just aft of the joint between the metal nose and plastic afterbody where the nose threads ended.

Three more models using cordwood-VVC transmitters and ruggedized Type B gages were constructed and launched. There was no output in flight on the first launch, shot 2886. However, launch or sabot-stripping peculiarities were present, as evidenced by the surface irregularities seen in the front-light laser photograph in Fig. 17. Although the cause of these irregularities cannot be positively identified, it is felt to be a result of particles from the sabot stripping operation impacting the model. The pin protruding from the rear of the model in Fig. 17 is for determining model roll orientation in flight. Also seen in Fig. 17 are the ink markings identifying the particular model (DM-11).

Heat-transfer data were acquired from the next two launchings, shots 2919 and 2920, but a comparison of the telemetered heat-transfer data to predicted values was more difficult than anticipated. First, a combination of unwanted transmitter frequency shift during both launches, and limited receiver bandwidths, necessitated complete post-shot recalibration of the receiving and recording systems in order to interpret the telemetered data. Second, the cone models were pitching, yawing, and rolling during both of these shots. It had been hoped that attitude variations would be minimal, so that the predicted model heat-transfer rates would be essentially constant. However, pitch and yaw angles varied between ±4 deg, with roll rates on the order of 0.3 deg/ft; this greatly influenced, and considerably complicated, the determination of the predicted heat-transfer rates. Analytical flow-field solutions were, therefore, computed for the particular model, model attitudes, and Range G shot conditions used,

by means of the techniques described in Refs. 9, 10, and 11. These analytical data were used to predict the heat rates existing at the gage locations on the model surfaces, establishing a basis for comparison with the telemetered data.

SECTION VIII
DISCUSSION OF HEAT-TRANSFER DATA

8.1 PREDICTED HEAT-TRANSFER DATA

At the conditions under which these two models were launched -- namely, a nominal Mach number of 6.0 and a nominal free-stream pressure of 50 torr -- predictions based on the methods described in Ref. 9 show the expected heat-transfer rate at the gage location to be near 30 Btu/ft^2-sec in laminar flow at zero angle of attack. However, neither model went through a zero attitude condition throughout flight. As an example, demonstrated by Fig. 18, the attitude data from each shadowgraph station are plotted for shot 2920 and connected by a solid line. The data for shot 2919 are similar. The effects of model roll are also illustrated in Fig. 18, where the orientations of the heat-transfer gage with respect to the pitch and yaw planes are shown at several shadowgraph stations. Heat rates predicted using the methods of Refs. 10 and 11 show that a 3-deg pitch angle will cause an increase in heat rate along a windward ray of about 33 percent; therefore, it is obvious from Fig. 18 that meaningful predictions of heat rates must take into account the model attitude information.

To predict instantaneous heat rates at the gage location as a function of time (or distance) during each flight, model attitude (roll, pitch, and yaw) was measured at each shadowgraph station. From these data, the roll orientation of the gage, with respect to the windward ray, could be determined. The characteristics plotted in Fig. 19, which arise from the analytical methods presented in Refs. 10 and 11, were then used to predict heat rate at the position occupied by the gage. (Model velocities decayed less than 1.3 percent during each flight and, therefore, were considered constant.)

The predicted instantaneous heat-transfer rates at the gage locations ($x/L = 0.694$) for shots 2919 and 2920 are shown in Figs. 20 and 21. These instantaneous heat rates were time-integrated to determine the heating experienced by the gage. These results are also shown in Figs. 20 and 21 (as are the values which would have resulted had yaw and pitch been zero). The gages (hence, the telemetry systems) were

assumed to respond exactly to these time-integrated curves. Slopes were taken over relatively linear portions of these curves, and the $\dot{q}$ values which resulted were used as a basis for evaluating the telemetered values (which were obtained by taking slopes over relatively linear portions of the experimental data).

8.2 TELEMETERED HEAT-TRANSFER DATA

The telemetry data were acquired using individual receivers covering three discrete segments of the Range G flight as described previously: (1) the blast chamber, (2) shadowgraph stations 1 to 14, and (3) shadowgraph stations 14 to 43. The receiver outputs were recorded on oscillographs for both shots, and also on magnetic tape for shot 2920.

It should be pointed out that the unwanted transmitter zero shifts which occurred during both launches would not necessarily have had deleterious effects upon telemetered data, if suitable receivers had been available for use. During shot 2919, for example, the zero shift (frequency shift) was approximately +300 kHz, and during shot 2920, it was about +400 kHz. Because one of the wide-band (3.3 MHz) receivers was required to monitor the frequency corresponding to an open-circuited gage during these shots, narrow-band receivers were used for two of the data channels (blast chamber, and Stations 1 to 14). For these two shots, the zero shifts described above caused the narrow-band receivers to operate where their discriminator characteristics are nonlinear, necessitating post-shot recalibration. These receivers require about 60 microvolts input for satisfactory operation (Table I). During flight, the incoming signal level dropped below this value on some occasions, degrading the accuracy with which the aerodynamic data could be interpreted.

After these launches, an investigation (described in Appendix IV) indicated that the large transmitter zero shifts during launch probably resulted from failure of the large-valued glass capacitors used as RF bypasses in the telemetry circuitry. Replacement capacitors have now been evaluated which are more rugged and occupy only about 1/40 of the volume required by the glass capacitors. Their use should reduce, and perhaps eliminate, these zero shifts.

8.3 COMPARISON OF TELEMETERED AND PREDICTED DATA

The telemetered and predicted values of heat-transfer rates for shots 2919 and 2920 are compared in Figs. 22 and 23. Several facets

of the data in these figures merit some discussion. For example, the scarcity of telemetered data for shot 2919 is readily apparent in Fig. 22. For unknown reasons, the signal radiated by the transmitter during shot 2919 was of a very low power level; hence, satisfactory reception was possible only when the model was near the pickup stubs of the antenna systems. The lack of coverage between Stations 7 and 14 is also obvious from Figs. 22 and 23. This is traceable directly to the tube-type receiver used for the Stations 1 to 14 antenna system, and to the antenna system itself, which has always been poorer in performance than the downrange antenna system.

The telemetered heat-transfer rates in the blast chamber over the first four or five milliseconds (28 to 35 feet) for both shots were considerably higher than the values predicted from aerodynamic considerations. This high indication probably resulted from the effects of hot muzzle gases enveloping the model. These gases could have actually produced a high heat rate, but they also could have caused the transmitter to indicate a false heat rate as a result of flight through a medium whose conductivity and/or permittivity was appreciably different from that of air. Supporting this muzzle-gas supposition is the fact that the telemetered values were much closer to the predicted values during model flight through the latter half of the blast chamber, as seen in Figs. 22 and 23.

The telemetered data received by the uprange antenna system (shadowgraph stations 1 to 14) for shot 2919 indicate an average heat rate of 15.8 Btu/ft^2-sec, whereas the predicted value is 18 Btu/ft^2-sec. The only downrange telemetered data which were acquired during this shot indicate 27.6 Btu/ft^2-sec, whereas the value predicted is 29.0 Btu/ft^2-sec over most of this same distance. Thus the telemetry system was indicating heat rates which were 5 to 12 percent below predicted values for this shot.

One of the front-light laser photographs (Fig. 24) shows that the gage was recessed about 15 mils below the model surface for shot 2919 during flight. (It had been flush with the model surface when loaded into the gun for launch.) Recession of the gage easily could result in discrepancies of the levels discussed but no effort was made to account for that factor. Analytical flow-field solutions for the case of laminar flow over a smooth body were used as a standard for comparison.

It is difficult to imagine how the gage became recessed without incurring some damage. Some model damage, indeed, may have occurred. As seen in Fig. 25, the plastic screw-in plug which contains the telemeter package can be seen protruding slightly from the rear of

the model. (This plug was machined flush with the model base after assembly.)

The telemetered data for shot 2920 are not in as good agreement with predicted values as for the previous shot (Fig. 23). A close examination of the real-time oscillograph record and the tape playback shows that several abrupt and random (but small) step changes occurred in the data traces throughout flight. As a result, if an "average" (straight line) slope is faired through all the data received between Stations 14 and 43, both the real-time and playback data indicate relatively low heat rates (11.6 and 16.0 Btu/ft^2-sec, respectively). However, if the experimental data are examined carefully, and the data reduced only over those portions of the range flight where no abrupt changes occurred in the data traces, and where the data slopes were relatively constant, the heat rates plotted in Fig. 23 result. During flight between Stations 20 and 30, for instance, where the predicted heat rate was constant, four separate slope reductions of experimental data indicate a heat rate of about 23.5 Btu/ft^2-sec, as can be seen in Fig. 23. This value is about 25 percent below the predicted value.

In at least three instances in Fig. 23, large disagreements may be seen between the indications from the real time and from the tape playback data. This is felt to result from the different frequency response characteristics of the recording systems used. Overall frequency response of the entire reception system during real-time recording was limited by galvanometer characteristics, and was typically 0 to 1.0 kHz. However, when recording this same information on the magnetic tape, the overall reception system response was on the order of 0 to 40 kHz. Thus, contributions from high frequency components (including extraneous, unwanted, signals) may have appeared during playback of the tape-recorded telemetered information, since playback was performed to provide an effective time expansion (32:1). These differences between data acquisition systems are felt partly responsible for the occasional, large disagreements in Fig. 23 between real-time and tape playback data and should be investigated further.

A possible source of anomaly associated with shot 2920 again has to do with model integrity. A laser photograph taken during this shot is shown in Fig. 26 and illustrates the point. The satin or frosted appearance of a model's surface has been observed during previous Range G shots; however, shot 2920 was the first where this effect was so pronounced. By way of comparison, the gage detail can be seen quite clearly in Fig. 25, as has been the case during previous telemetry shots. A depression of unknown origin in the model surface can also be seen in Fig. 26, running from the gage toward the base of the model.

Because of instrumentation malfunction, no laser photographs which would allow determination of whether or not the gage was recessed were recorded during shot 2920.

SECTION IX
CONCLUDING REMARKS

Even though the agreement between telemetered and theoretical heat-transfer rates was not as good as desired, the fact that data were received at all was encouraging; it represented the first known successful acquisition of on-board aerodynamic data via telemetry from a two-stage launcher facility. The difficulty encountered in obtaining satisfactory telemetry operation using a two-stage launcher prompts the following observations:

1. The accelerations encountered during the two-stage launchings were lower in peak magnitude than those encountered during previous, successful, single-stage launchings; however, the accelerations persisted for much longer times in the two-stage application. In regard to the duration of the acceleration, it had been demonstrated statically that the transmitters could successfully withstand compressive loads more than ten times greater than the compressive loads expected as a result of gun launch; yet unpredictable shifts in transmitter frequency occurred during launch, if the transmitter operated at all. Thus, compressive stresses alone do not appear to cause the transmitter malfunctions or failures observed in Range G launchings.
2. The model structure apparently failed in tension during shot 2812, pointing out the likelihood that tensile waves propagated through the structure during launch. Tensile waves could have disastrous effects on the glass capacitors used; and capacitor failure could cause the anomalous transmitter behavior (failure to operate, or large, unpredictable zero shifts) observed during these two-stage launches. During previous single-stage launchings at higher peak accelerations, transmitters seldom failed to operate, and large transmitter frequency shifts were absent. However, the single-stage launches generally were made with the telemetry systems contained in

cylindrical models. Thus, it remains to be determined whether the tensile failure arose from the use of a two-stage launcher, or from the use of a different test model, or both.

Static compression tests and dynamic impulse tests of the kind performed here cannot fully simulate the complex structural loading imposed on the model by the two-stage launch cycle. However, these tests do provide relatively inexpensive means of simulating either compressive loads or peak accelerations for evaluation purposes. Furthermore, the test specimens generally are recoverable, allowing post-test diagnoses as to what specific component might have failed. Successful system operation throughout static compression and dynamic impulse tests should not be construed as evidence that a system will perform satisfactorily after a two-stage launch. However, failure to survive these static compression tests and dynamic impulse tests should be interpreted as predictions of failure in the two-stage launcher.

The effects of model pitch, yaw, and roll have been incorporated into a theoretical program for predicting surface heat-transfer rates. This theoretical model provides a credible reference with which the experimental telemetry data may be compared. However, it is clear that a pitching, yawing, and rolling cone model is not the ideal test vehicle in which to evaluate the telemetry system, because the heat-transfer rate at the gage location is not constant. At present, the transient response of the gage has been investigated only for the assumed case of a step input of the proper magnitude, followed by a sinusoidal variation in heating as a result of simple model oscillation. Still to be investigated are: (1) possible effects on data telemetered subsequent to exposure of the gage to an extremely high heat rate, such as might be experienced early in the blast chamber during a Range G telemetry shot (Figs. 22 and 23); and (2) the transient response of the gage to a non-sinusoidal input such as shown by the predicted rates in Figs. 20 and 21.

In summary, heat-transfer data were obtained during two consecutive launchings. Data agreement with predicted values was not as good as expected, probably a result of a combination of the following factors: (1) discrepancies in predicting the transient $\dot{q}$ values which resulted from model attitude variations; (2) incorrect assumption that the gage follows the $\int \dot{q}\, dt$ curve exactly; and (3) degradation of data resolution and accuracy by low signal levels, and by nonlinear receiver operation.

One of the weak links in regard to heat-transfer telemetry -- namely, the one causing the large zero shift -- was tentatively identified

in laboratory tests subsequent to the two launches mentioned above. A glass capacitor invariably failed first, and produced a large shift in telemeter frequency, during static compression tests. As described in Appendix IV, a capacitor performing one particular function appears particularly susceptible to early failure; and failure of this capacitor would produce the large, unpredictable zero shifts observed, as discussed in Section 6.2. Uncased, ceramic capacitors, which were acquired and static-compression tested, appear clearly superior to glass capacitors for gun-range tests, and will be evaluated in any future range telemetry applications.

Better resolution is required in the telemetry readout instrumentation. The presence of noise in the data trace can mask small changes in data slope (heat rate), yet relatively high frequency response is required to provide fast rise times in transient applications such as these. The data frequencies should be relatively low, since the frequency of model oscillation is on the order of 25 Hz. If the rise time requirement could be disregarded, an overall system response of 0 to 50 Hz would probably be adequate, assuming simple model motion. Some preliminary work has been done in playing back the data tapes through low-frequency galvanometers (0 to 25 Hz), and through very low-frequency filters (0 to 0.5 Hz). Though not enough results have been obtained to make firm recommendations at this time, it appears quite possible to establish a realistic tradeoff between frequency response and rise time requirements such that noise effects on data can be substantially reduced.

Now that telemetry data have been obtained, the solid-state wideband receivers previously used to monitor certain telemetry failure modes could be used for $\dot{q}$ data acquisition. This would greatly reduce, and perhaps eliminate, data reduction complications resulting from transmitter zero shifts such as occurred during these two shots.

REFERENCES

1. Lukasiewicz, et al. "Development of Hypervelocity Range Techniques at Arnold Engineering Development Center (U)." Proceedings of ARPA-CARDE-ARGMA Symposium on Aeroballistic Ranges, June 28-29, 1961, Valcarter, P. Q., October 1961. Carde Technical Memorandum Q-646/61, pp. 75-142. Part 1 - Unclassified Technical Presentations.

2. Kingery, M. K., Choate, R. H., and Young, R. P. "Progress Report on Development of Telemetry for a Hypervelocity Range." AEDC-TN-60-214 (AD248019), December 1960.

3. Clemens, P. L. and Hendrix, R. E. "Development of Instrumentation for the VKF 1000-ft Hypervelocity Range." Proceedings of the 2nd Symposium on Hypervelocity Techniques, Denver, Colorado, March 1962.

4. Dugger, P. H., Enis, C. P., and Hill, J. W. "Laser High-Speed Photography for Accurate Measurements of the Contours of Models in Hypervelocity Flight within an Aeroballistic Range." Proceedings of Electro-Optical Systems Design Conference, New York Coliseum, September 22-24, 1970.

5. Choate, R. H. "Free-Flight Telemetry Instrumentation for Wind Tunnels." Proceedings of National ISA Aerospace Instrumentation Symposium, Las Vegas, Nevada, May 5-7, 1969.

6. Morgan, C. C., Jr. and Andrews, J. C. "Morgandyne Heat-Transfer Transducer and A Flame-Torch Calibration Technique for Hypervelocity Wind Tunnels." AEDC-TR-60-1 (AD232236), February 1960.

7. Ledford, R. L. "A Device for Measuring Heat-Transfer Rates in Arc-Discharge Hypervelocity Wind Tunnels." AEDC-TDR-62-64 (AD275740), May 1962.

8. Kuechle, Larry B. "Batteries for Biotelemetry and Other Applications." Telemetry, January-February, 1969, p. 19.

9. Adams, J. C., Jr. "Eddy Viscosity-Intermittency Factor Approach to Numerical Calculation of Transitional[2] Heating on Sharp Cones in Hypersonic Flow." AEDC-TR-70-210 (AD714058), November 1970.

10. Adams, J. C., Jr. "Finite-Difference Analysis of a Three-Dimensional Turbulent[2] Boundary Layer on a Sharp Cone at Angle of Attack in a Supersonic Flow." Presented at AIAA Tenth Aerospace Sciences Meeting, San Diego, California, January 17-19, 1972.

11. Adams, J. C., Jr. "Three-Dimensional Laminar Boundary-Layer Analysis of Upwash Patterns and Entrained Vortex Formation on Sharp Cones at Angle of Attack." AEDC-TR-71-215 (AD), December 1971.

---

[2]These data are shown therein to be applicable to the present, laminar flow case also.

APPENDIXES

I. ILLUSTRATIONS
II. TABLES
III. FM/FM TELEMETRY SYSTEM
IV. UNCASED, CERAMIC CAPACITORS

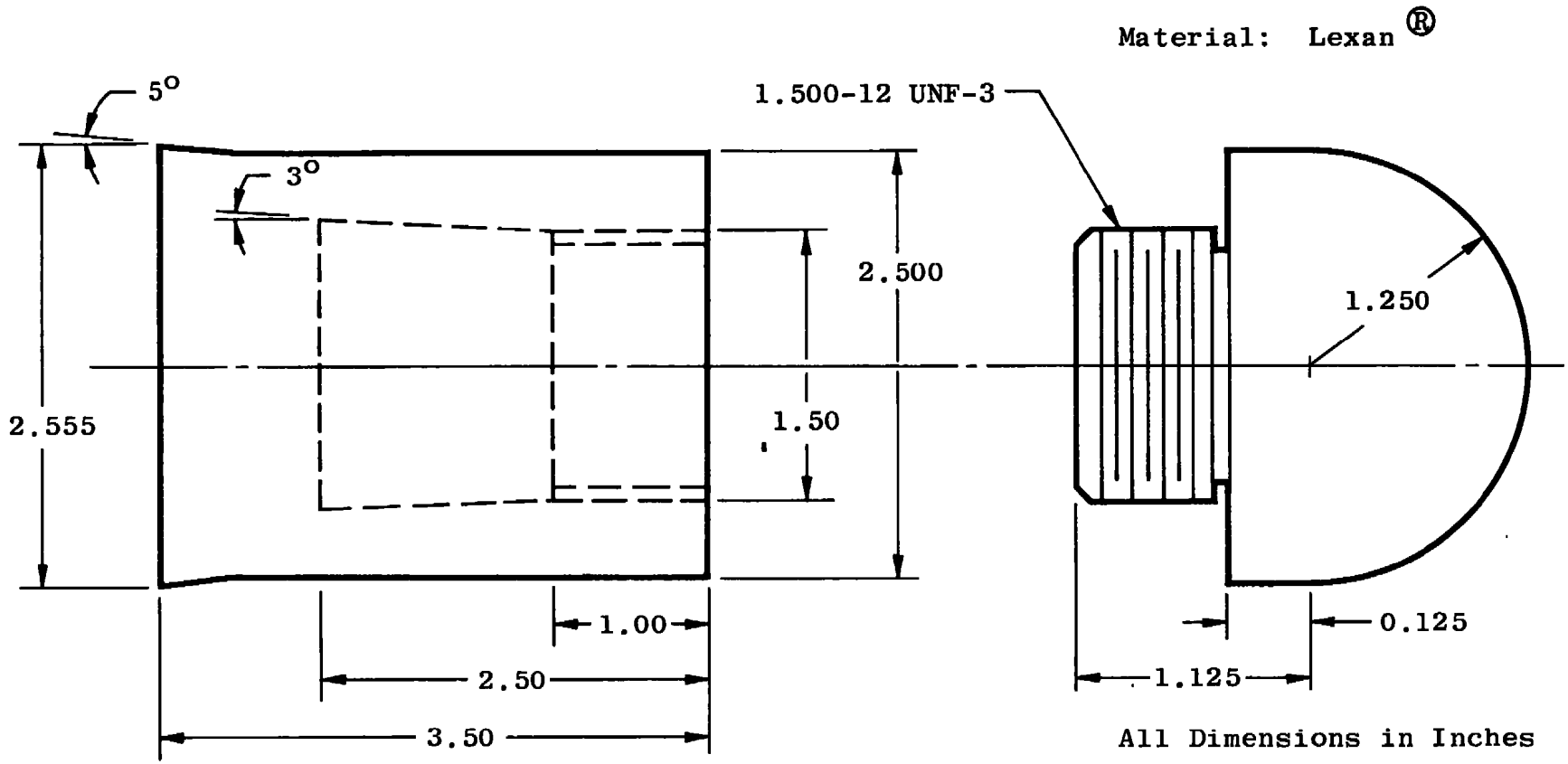

Fig. 1 Impulse Test Model

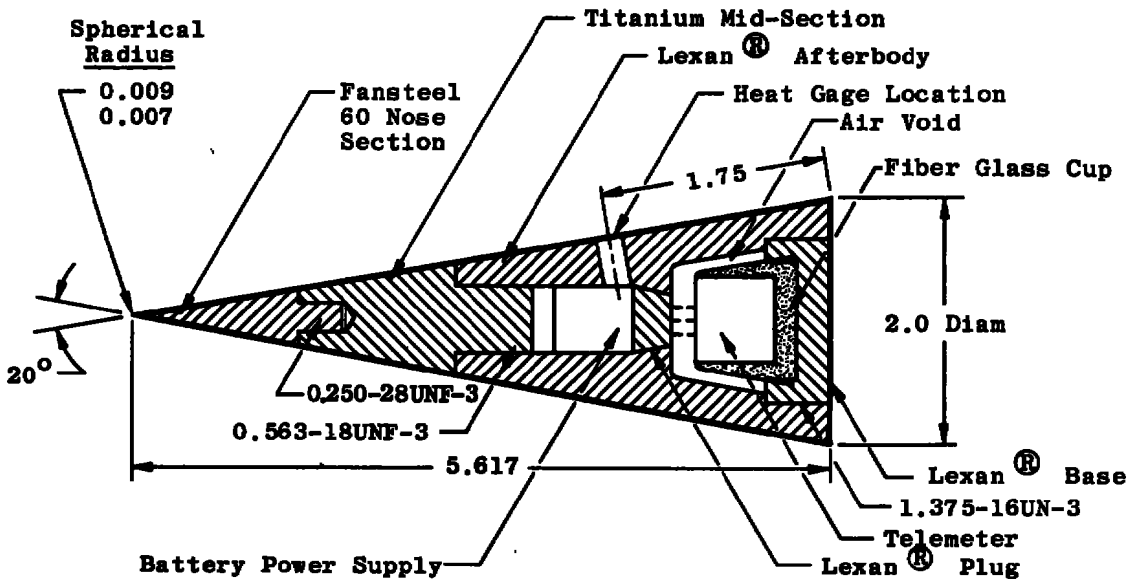

a. Plastic Model

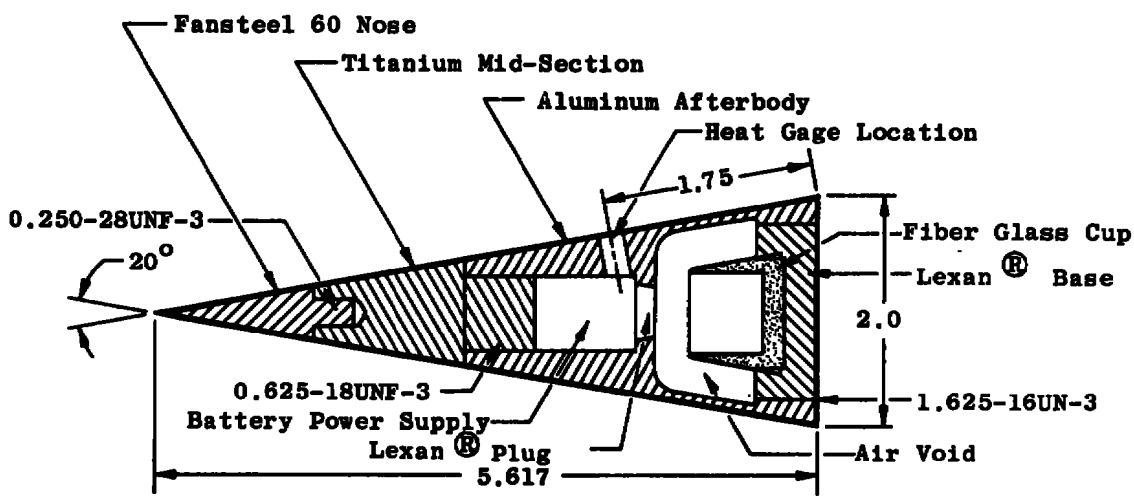

All Dimensions in Inches

b. Metal Model

Fig. 2 Range G Cone Models

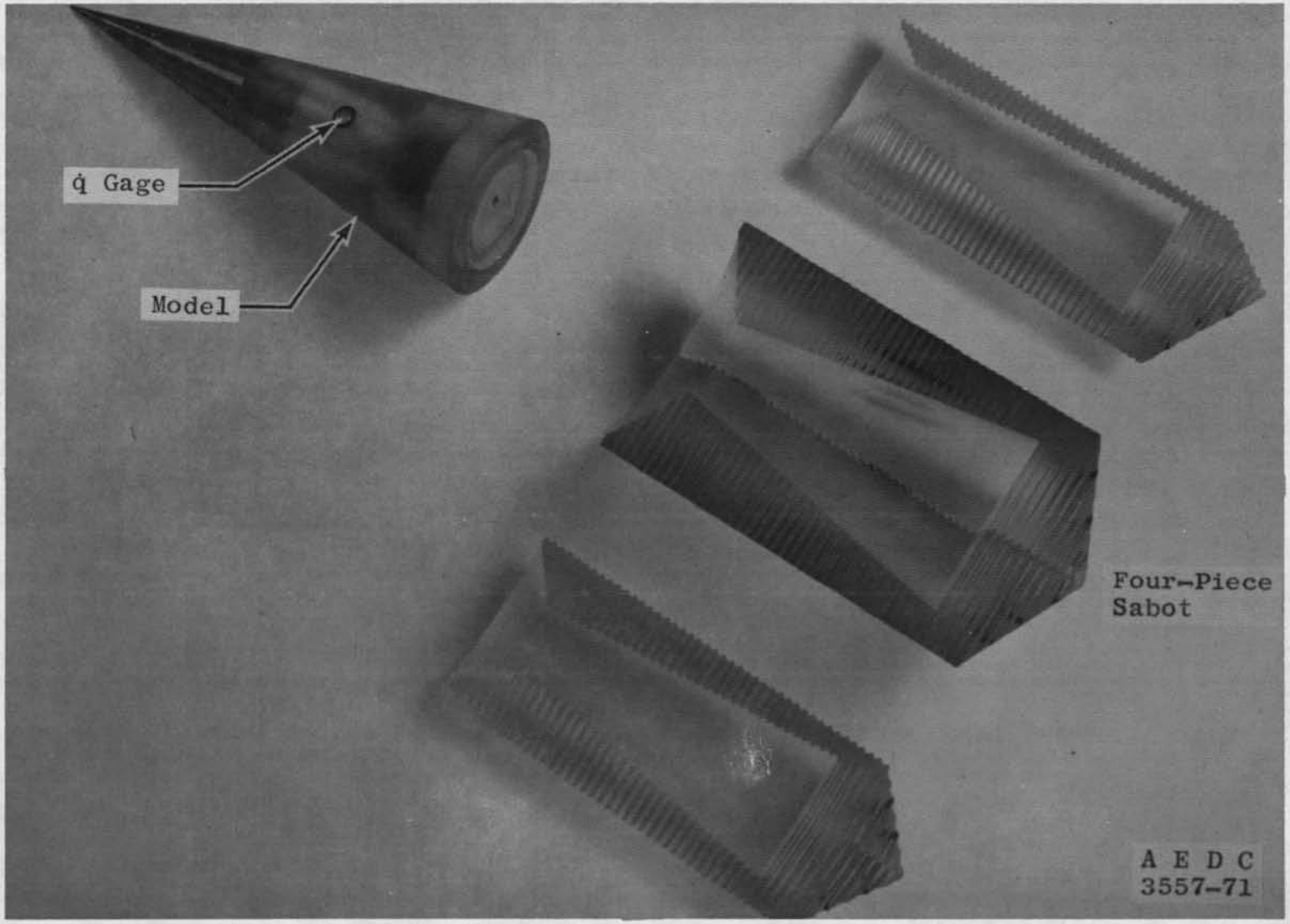

Fig. 3 Model and Sabot

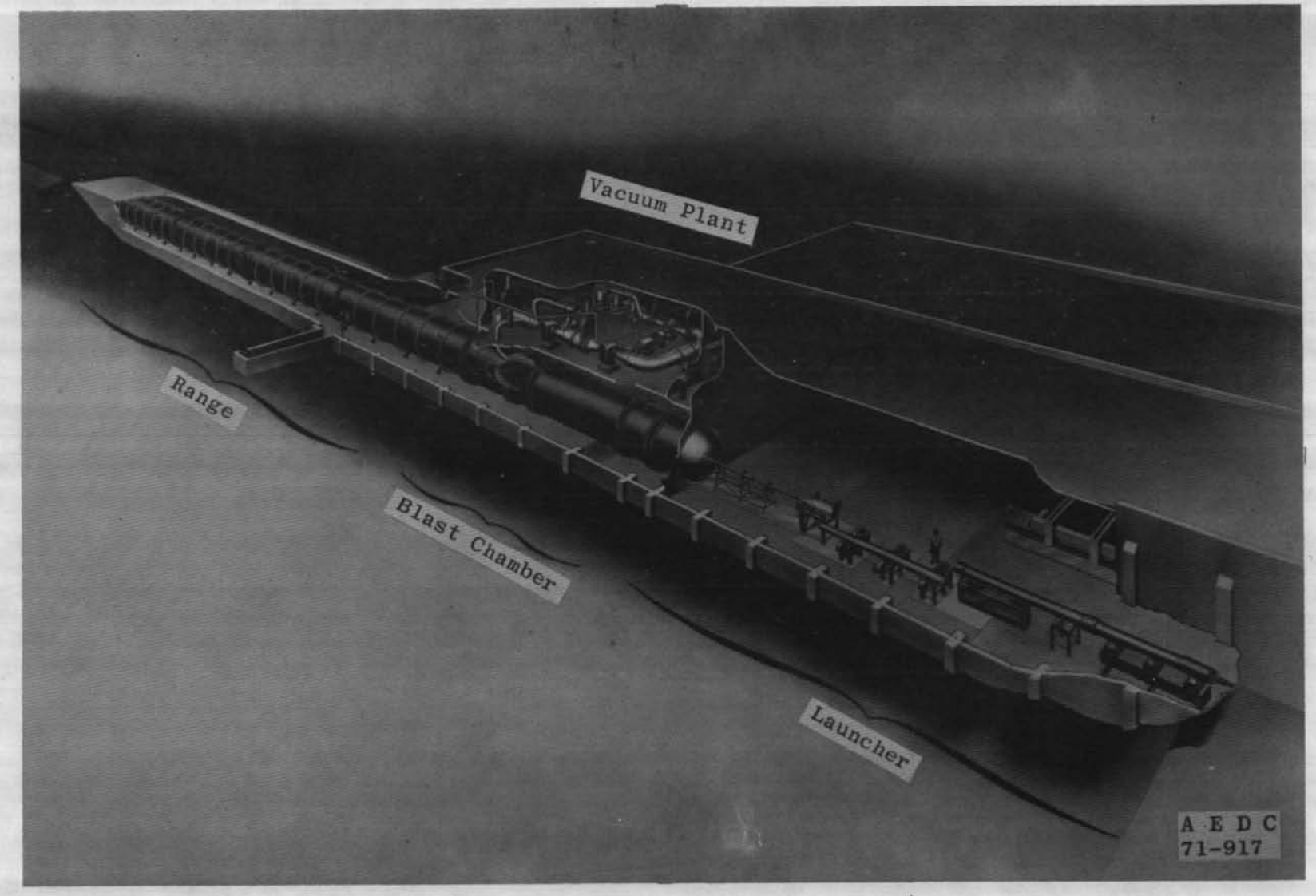

Fig. 4 VKF 1000-ft Hyperballistic Range (G)

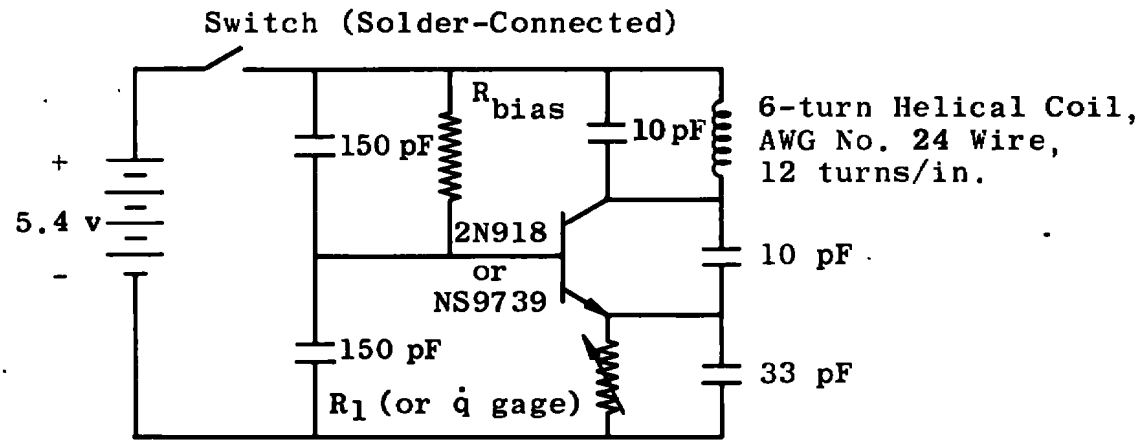

Fig. 5 Colpitts Oscillator, Variable Emitter Modulation

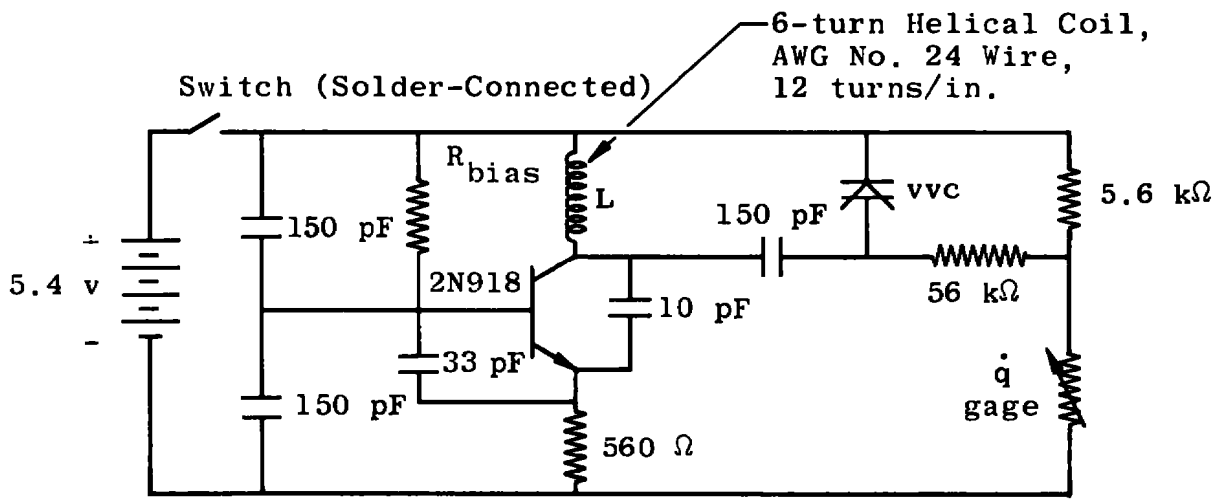

Fig. 6 Colpitts Oscillator, VVC Modulation

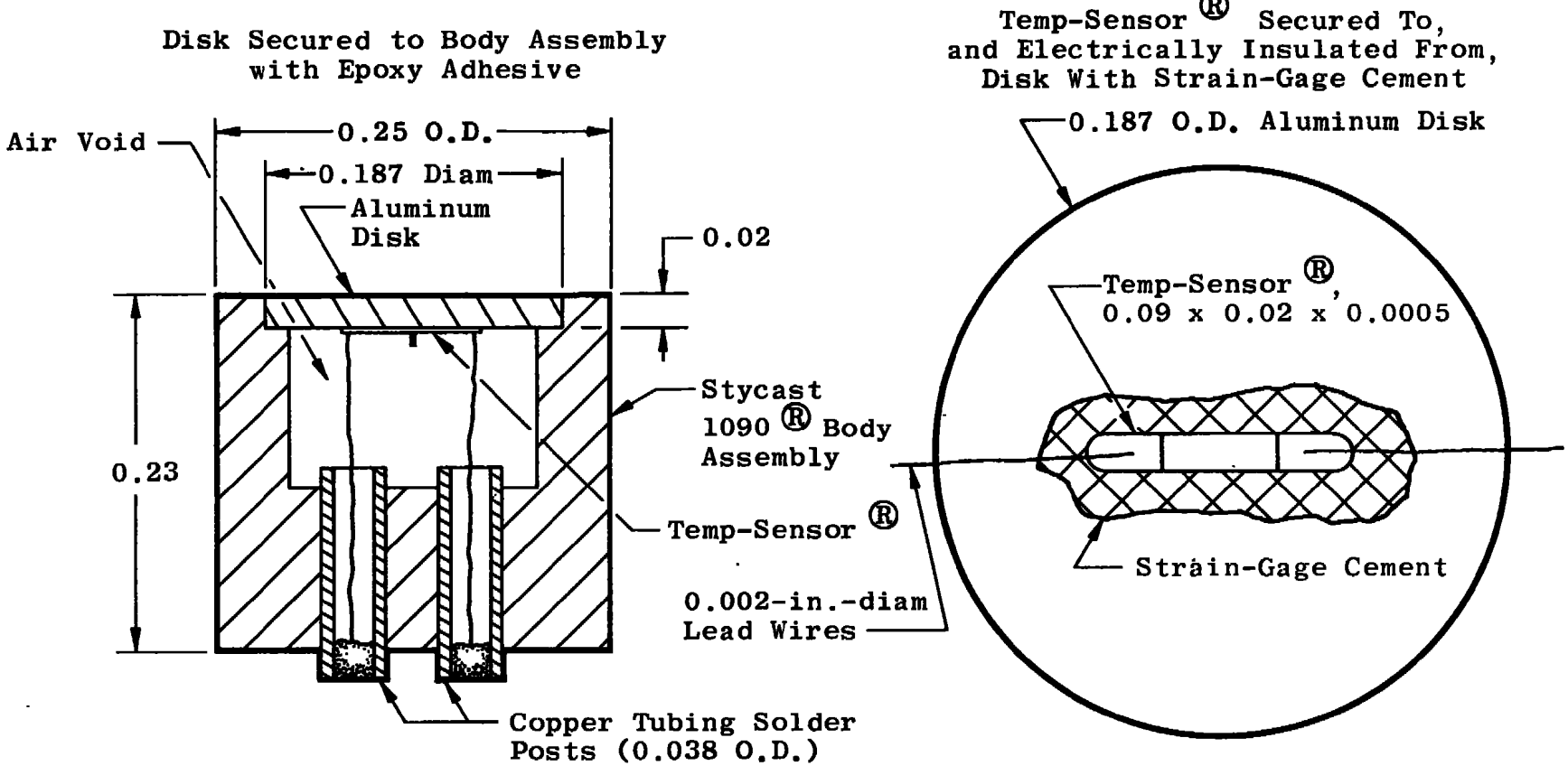

Transducer Assembly

10 x Scale

Back View of Sensing Disk

20 x Scale

Fig. 7 $\dot{q}$ Gage

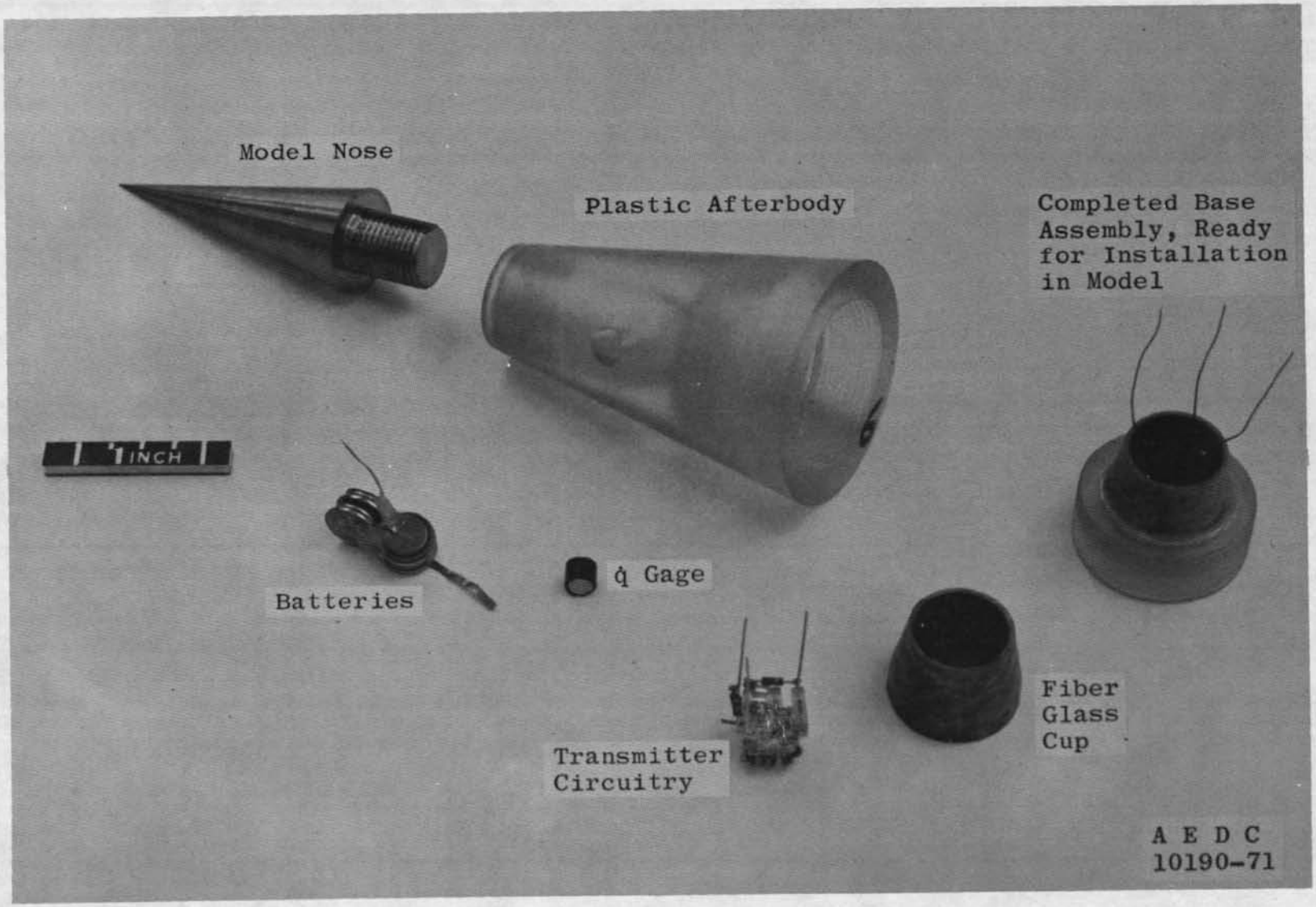

Fig. 8 Photograph of Telemeter Components

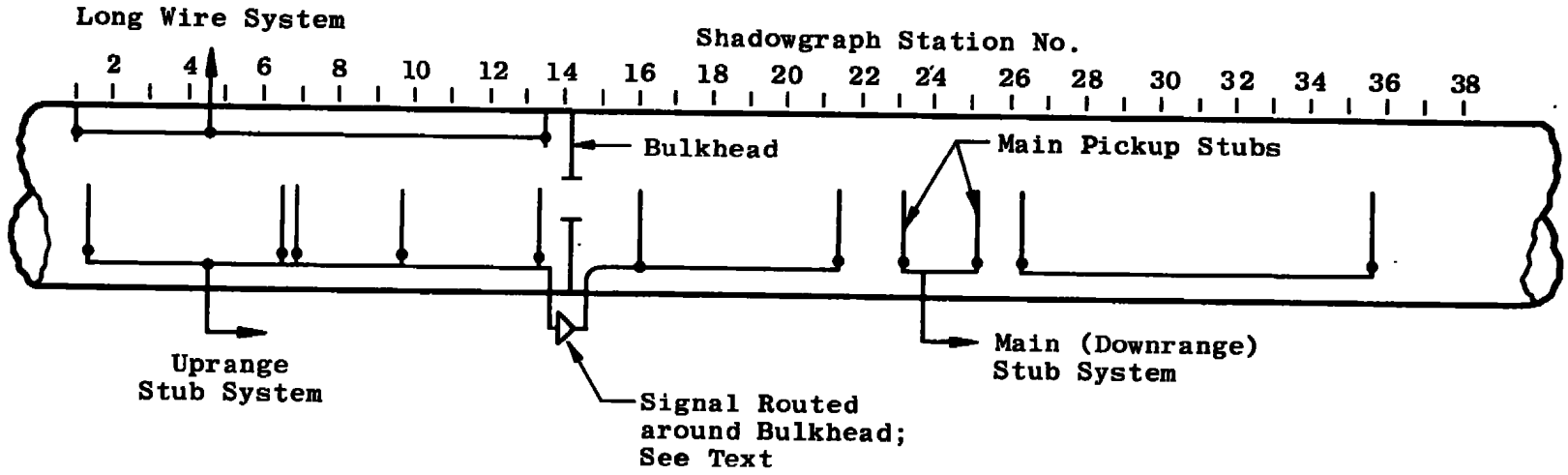

Fig. 9 G Range Antenna System

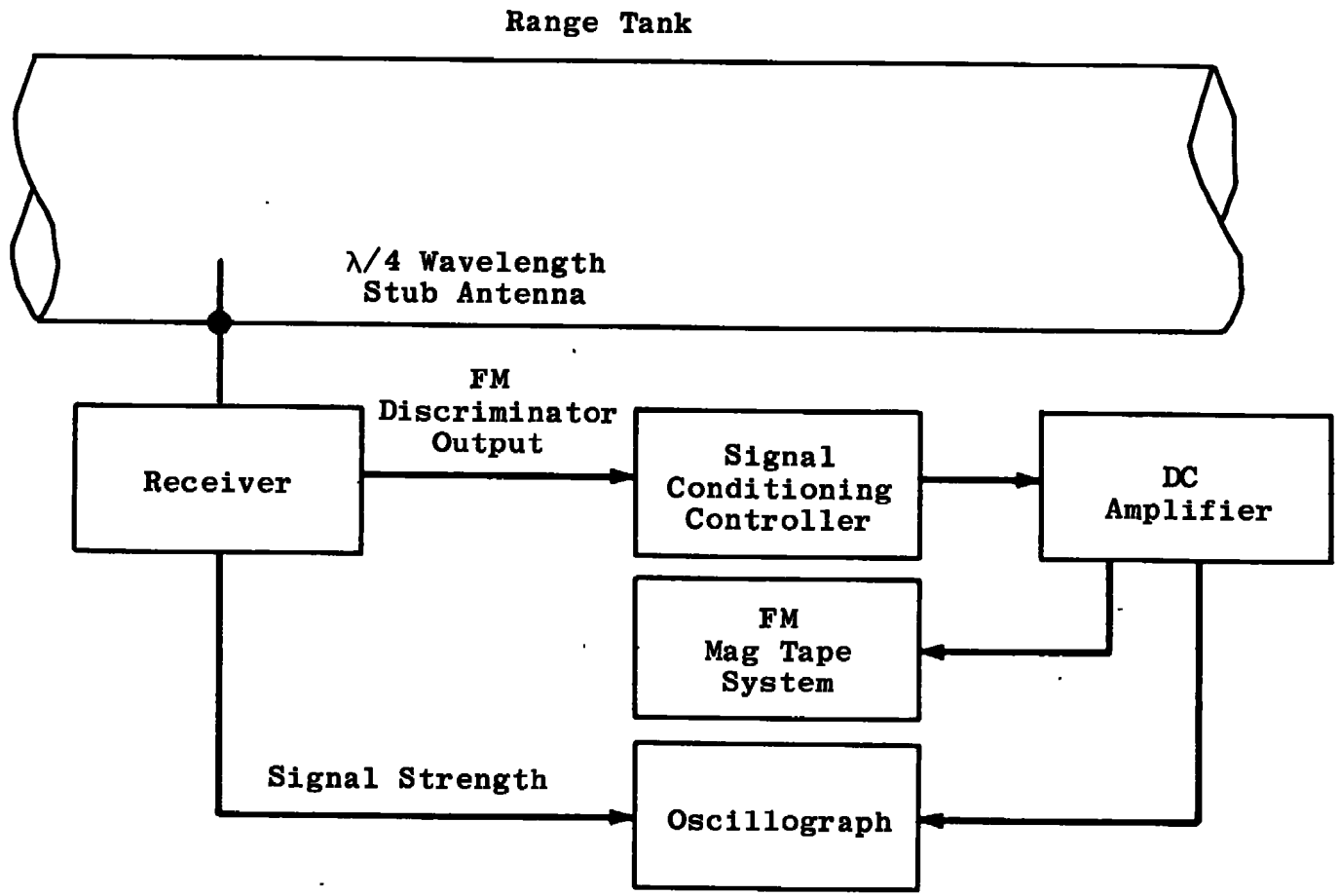

Fig. 10 Single-Channel Telemeter Data Acquisition System

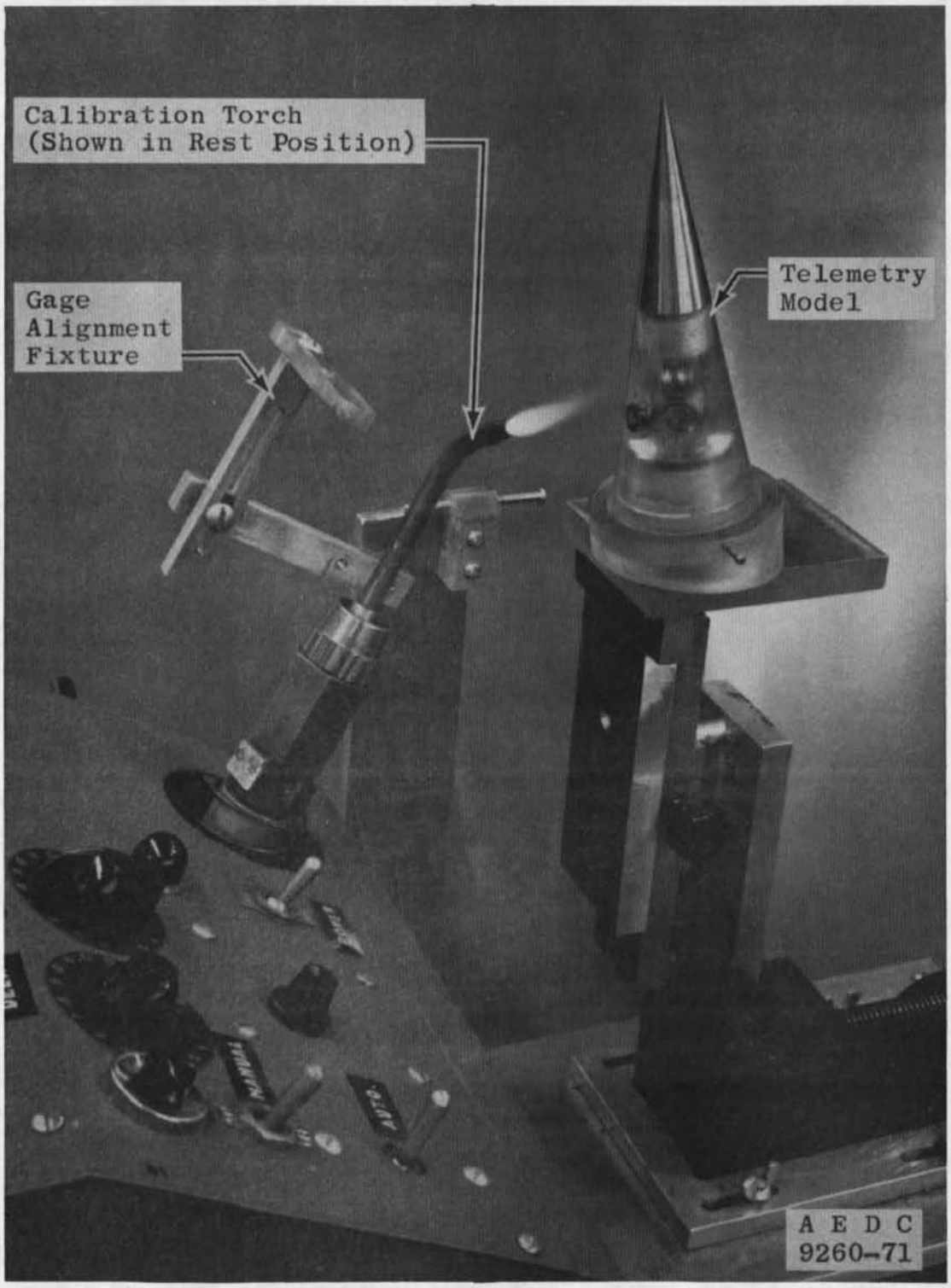

Fig. 11 Heat-Transfer Calibration Apparatus

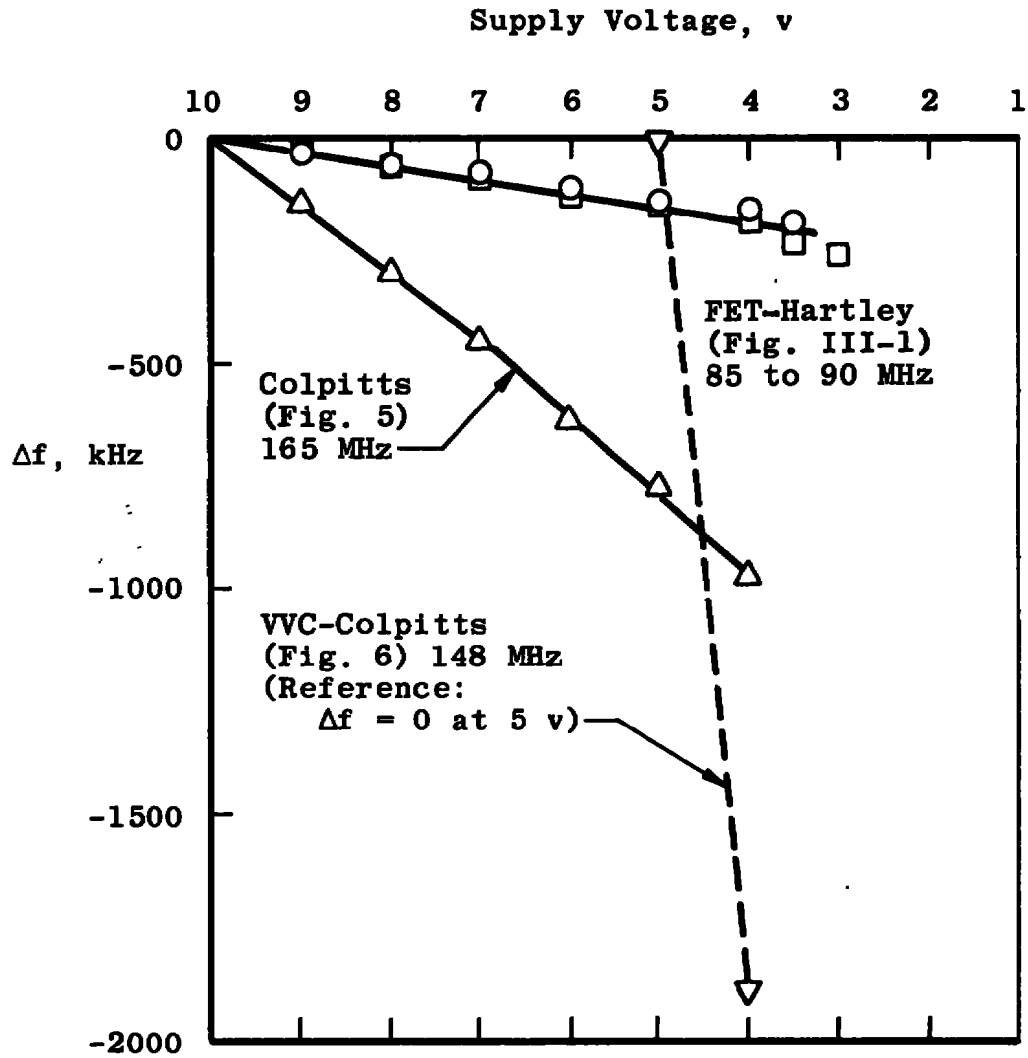

Fig. 12 Transmitter Voltage Sensitivities

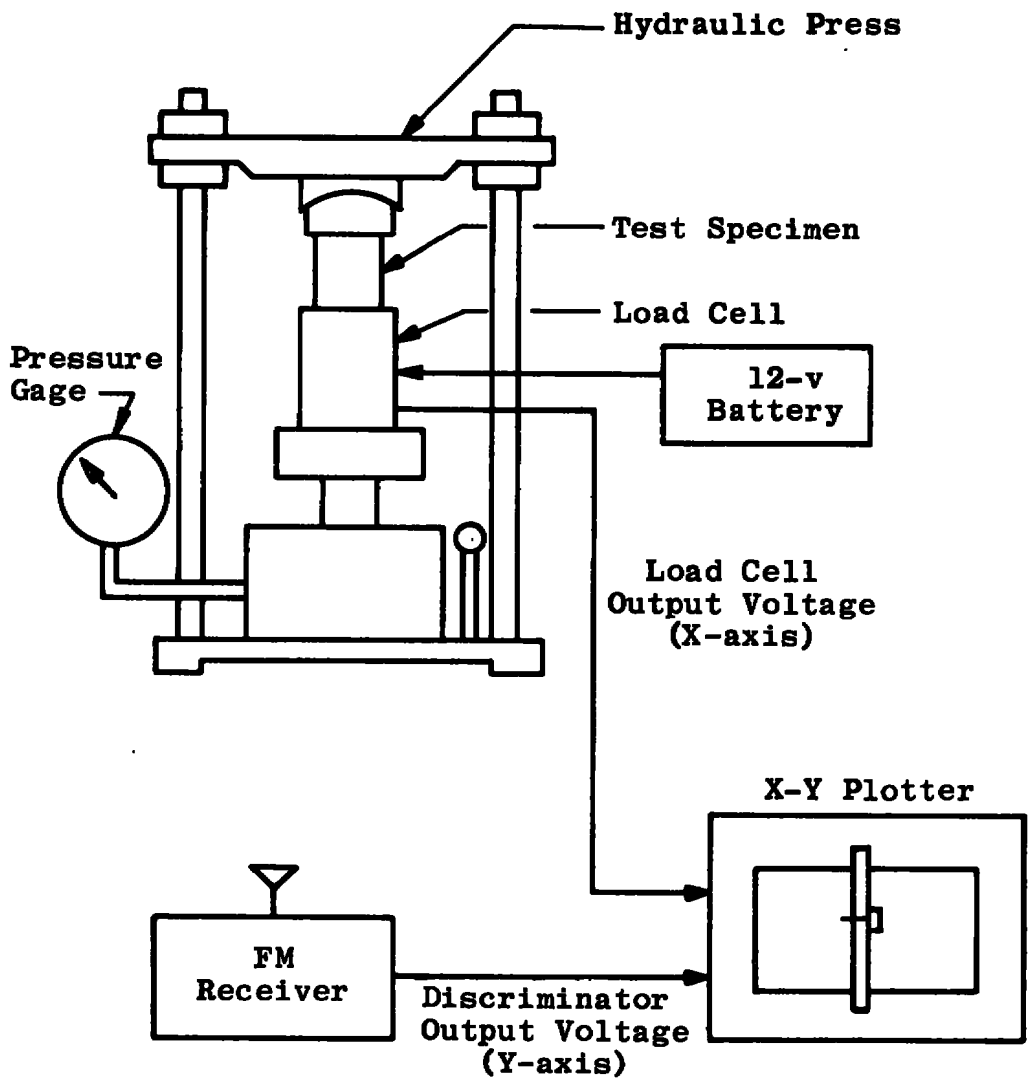

Fig. 13 Static Compression Test Apparatus

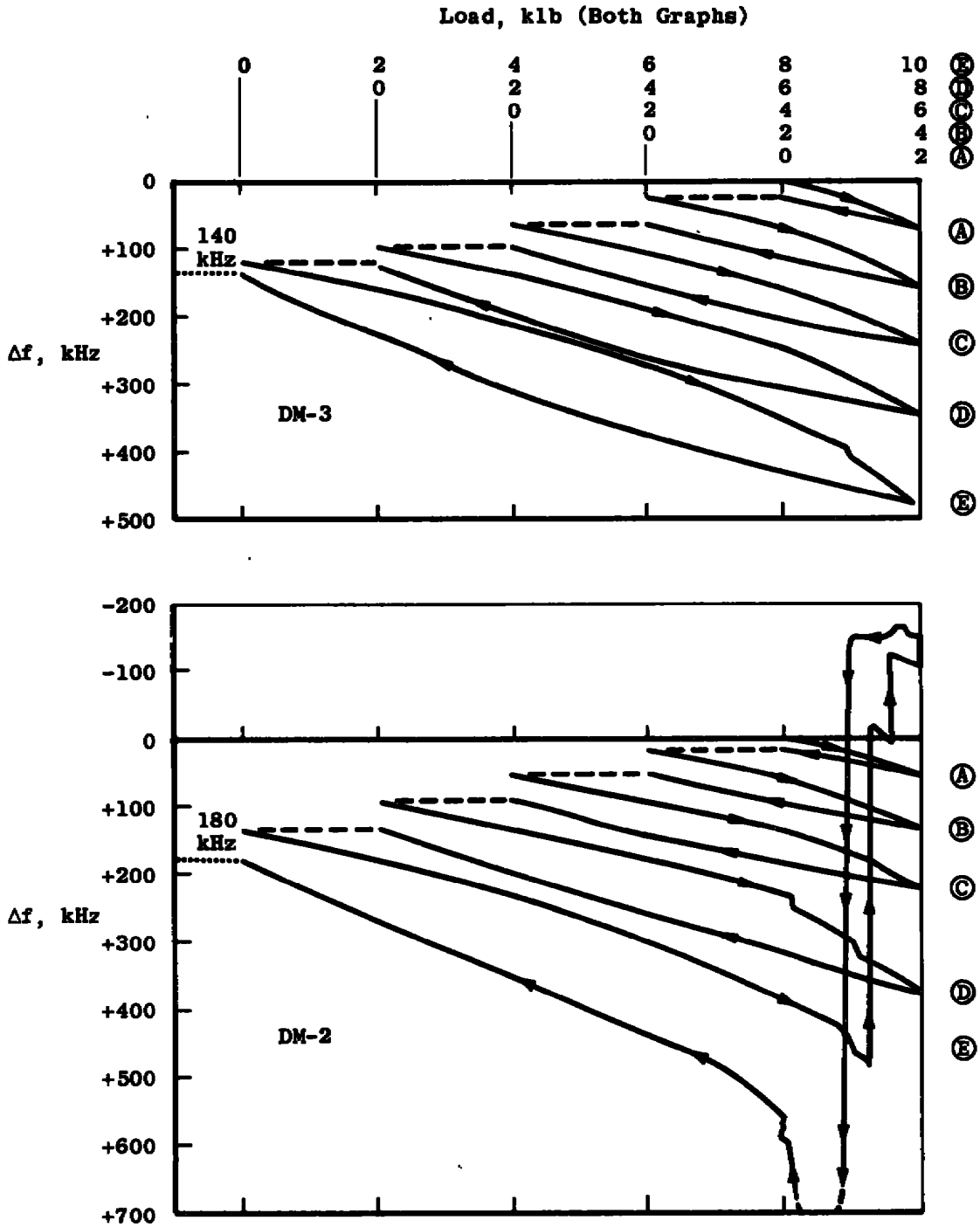

Fig. 14 Load-Frequency Characteristics

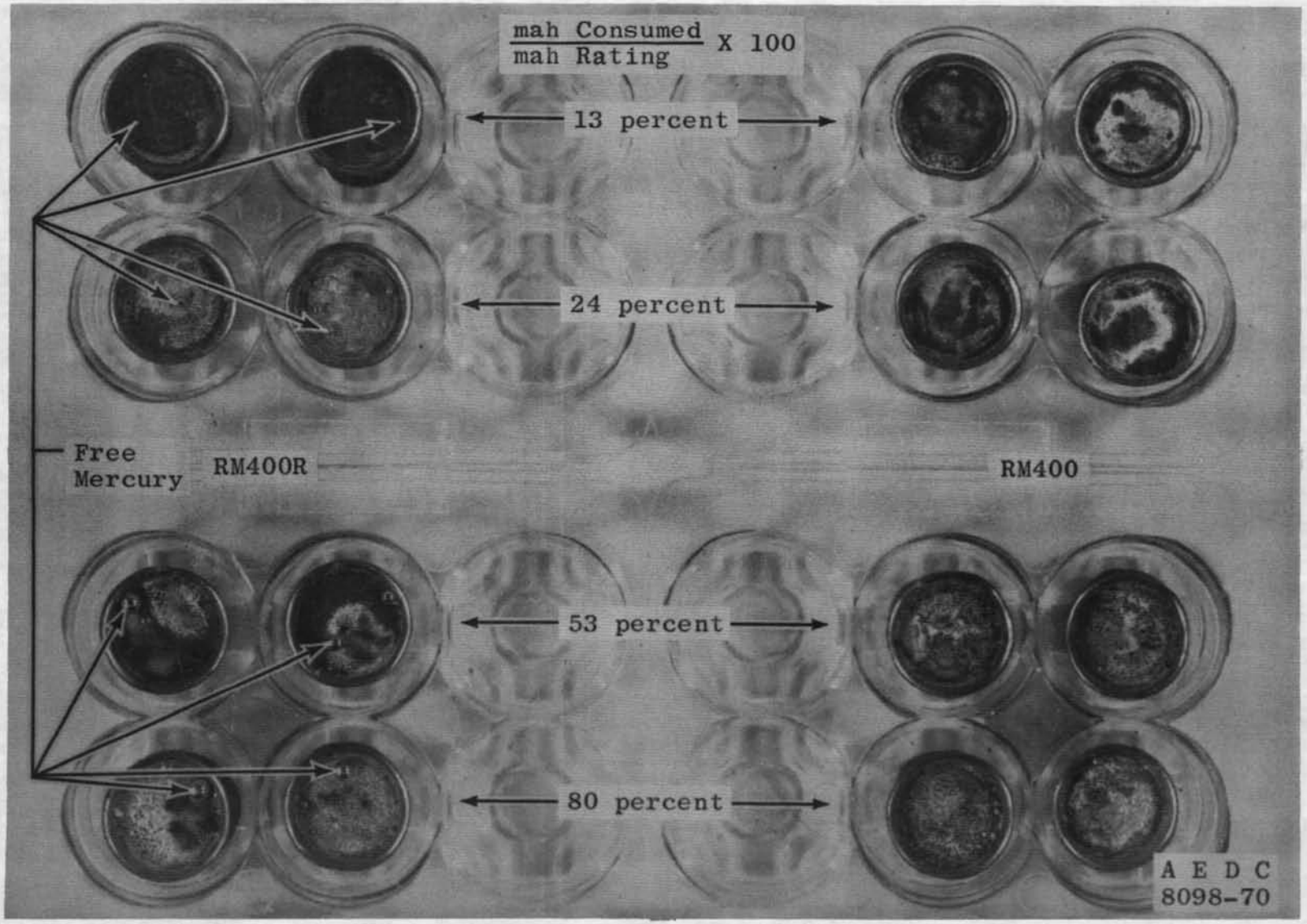

Fig. 15 Battery Comparison, Mercury Accumulation

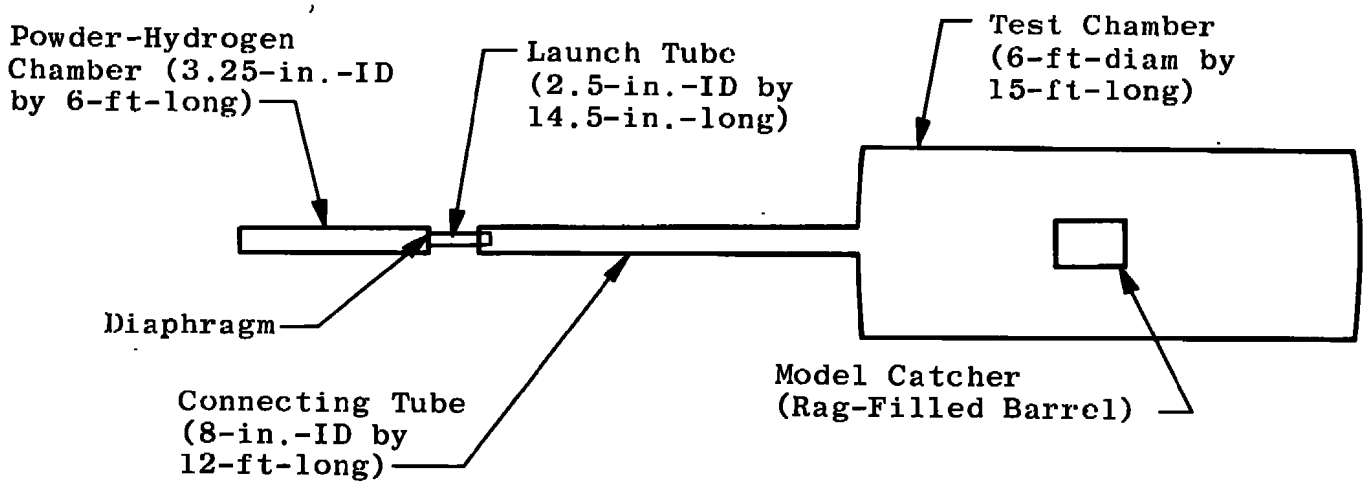

Fig. 16 Impulse Test Apparatus

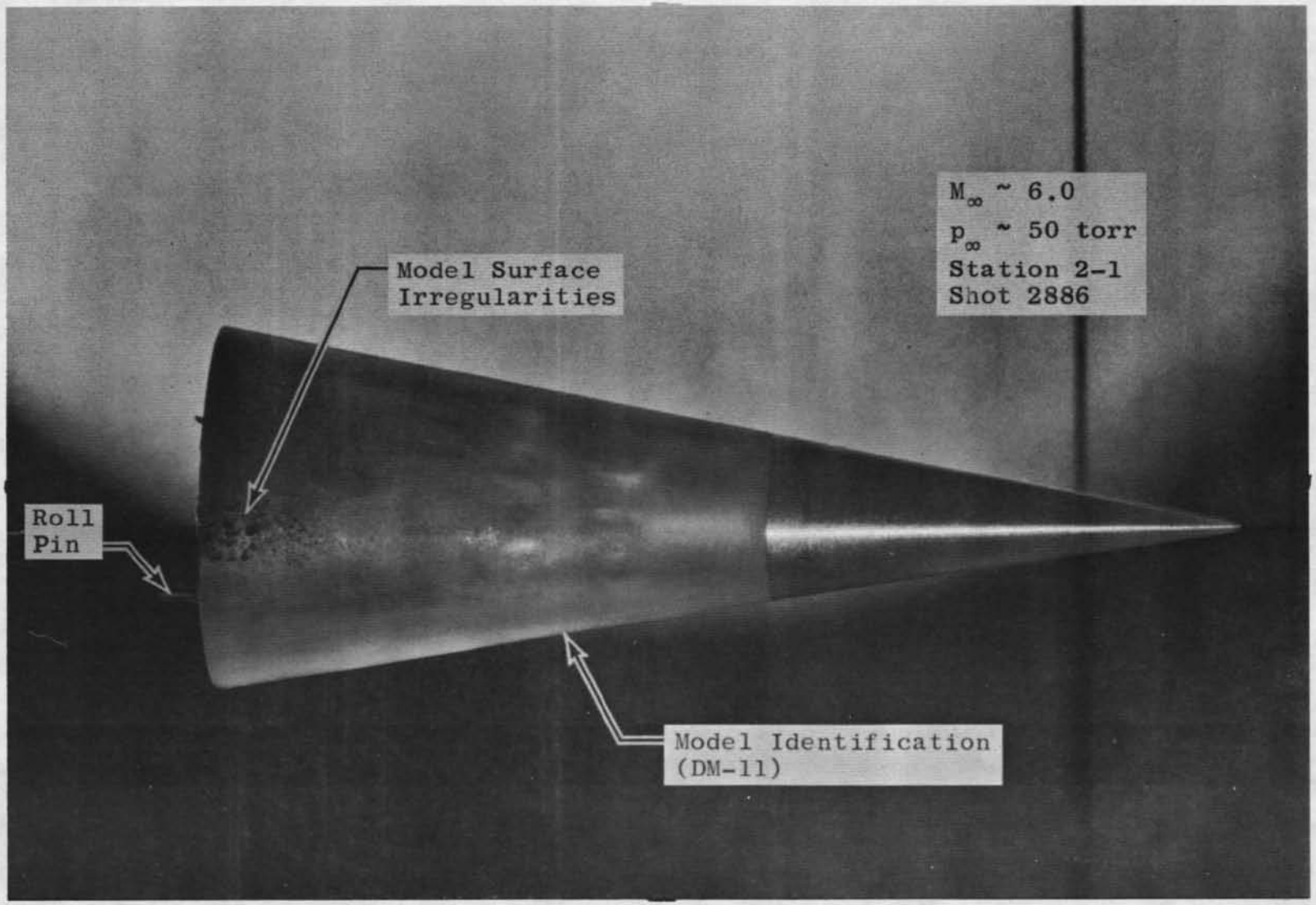

Fig. 17 Damaged Model, Shot 2886

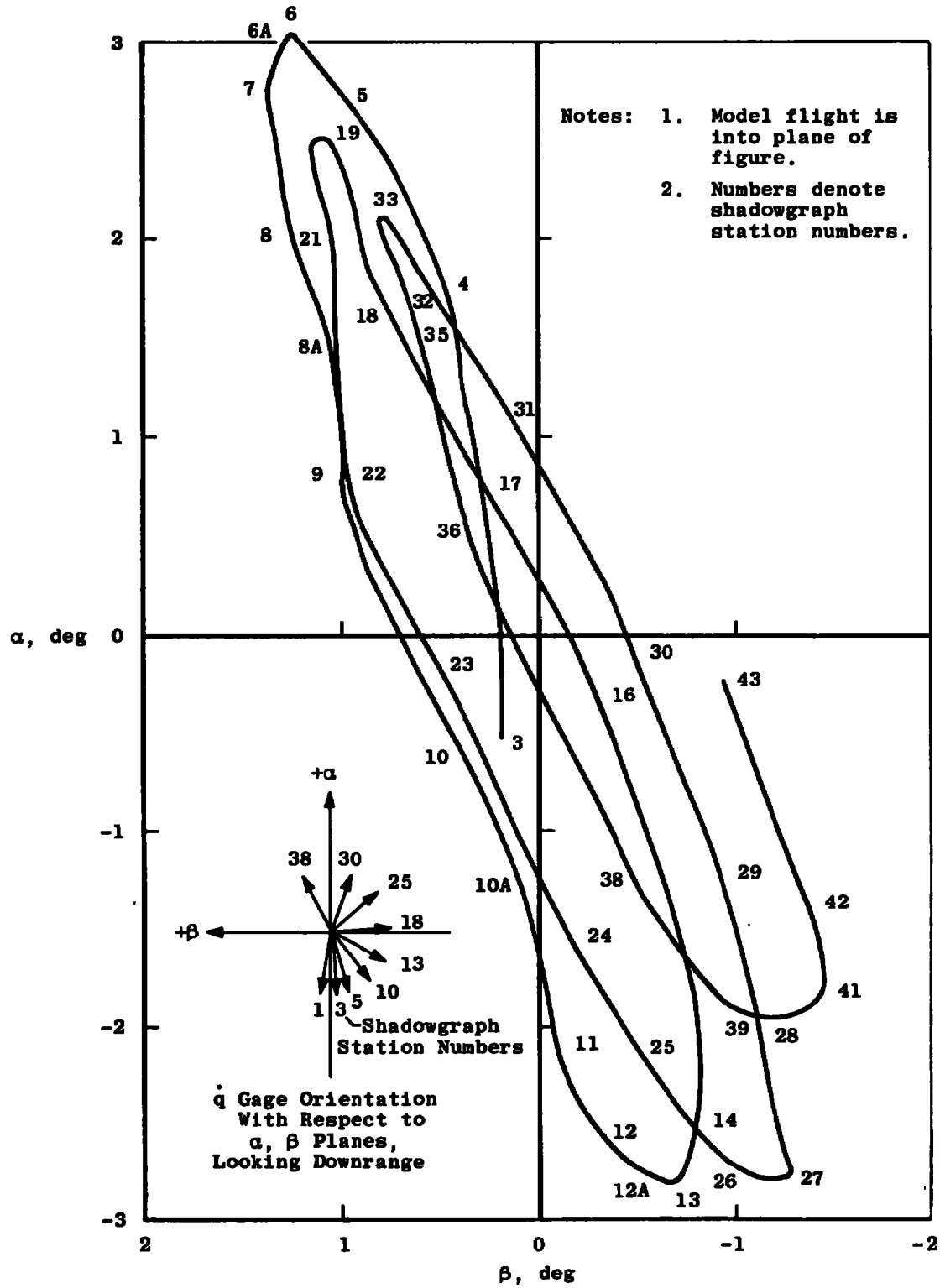

Fig. 18 Shot 2920 Attitude Variations

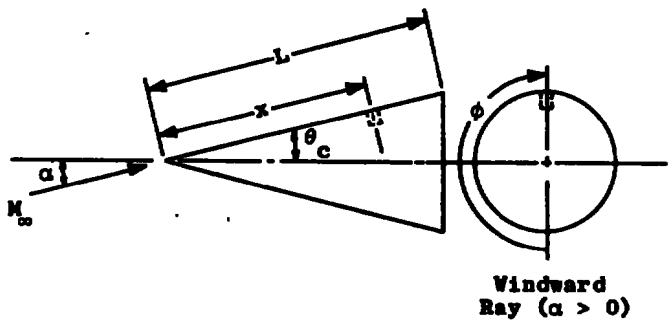

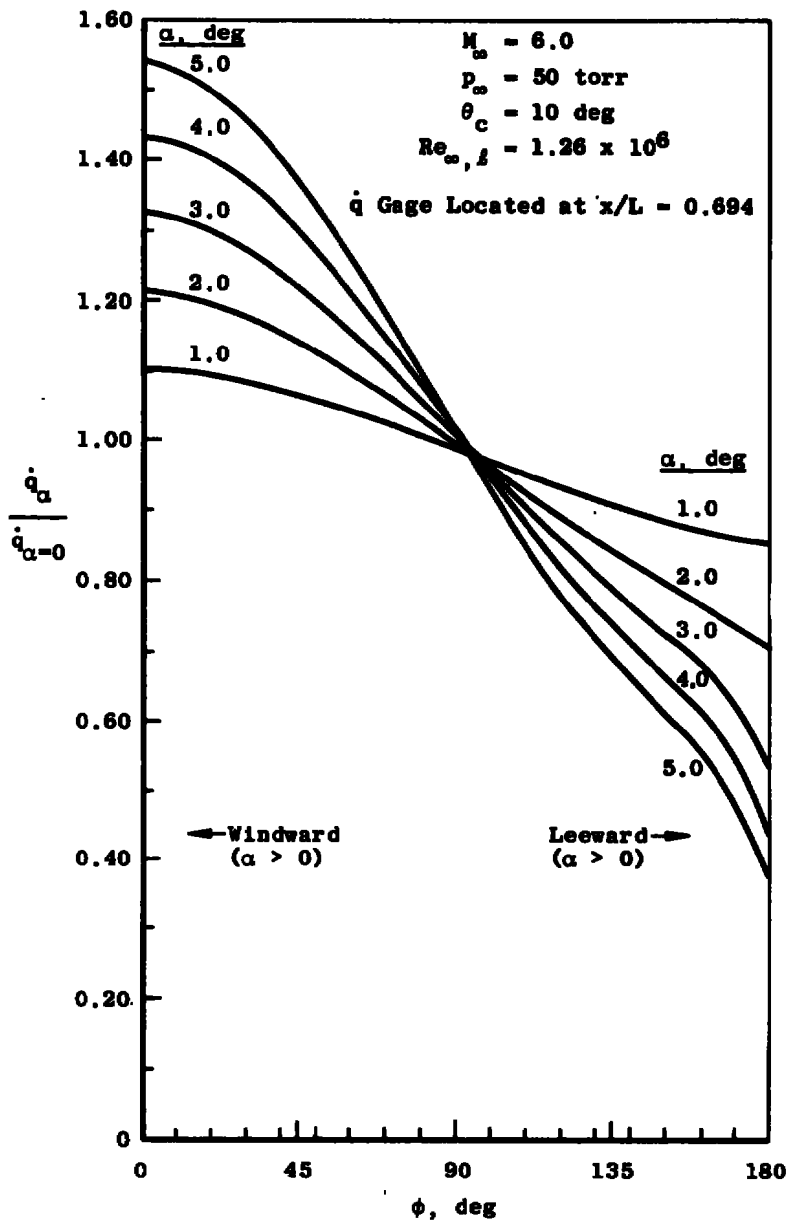

Fig. 19 Effects of Attack and Roll Angle on $\dot{q}$

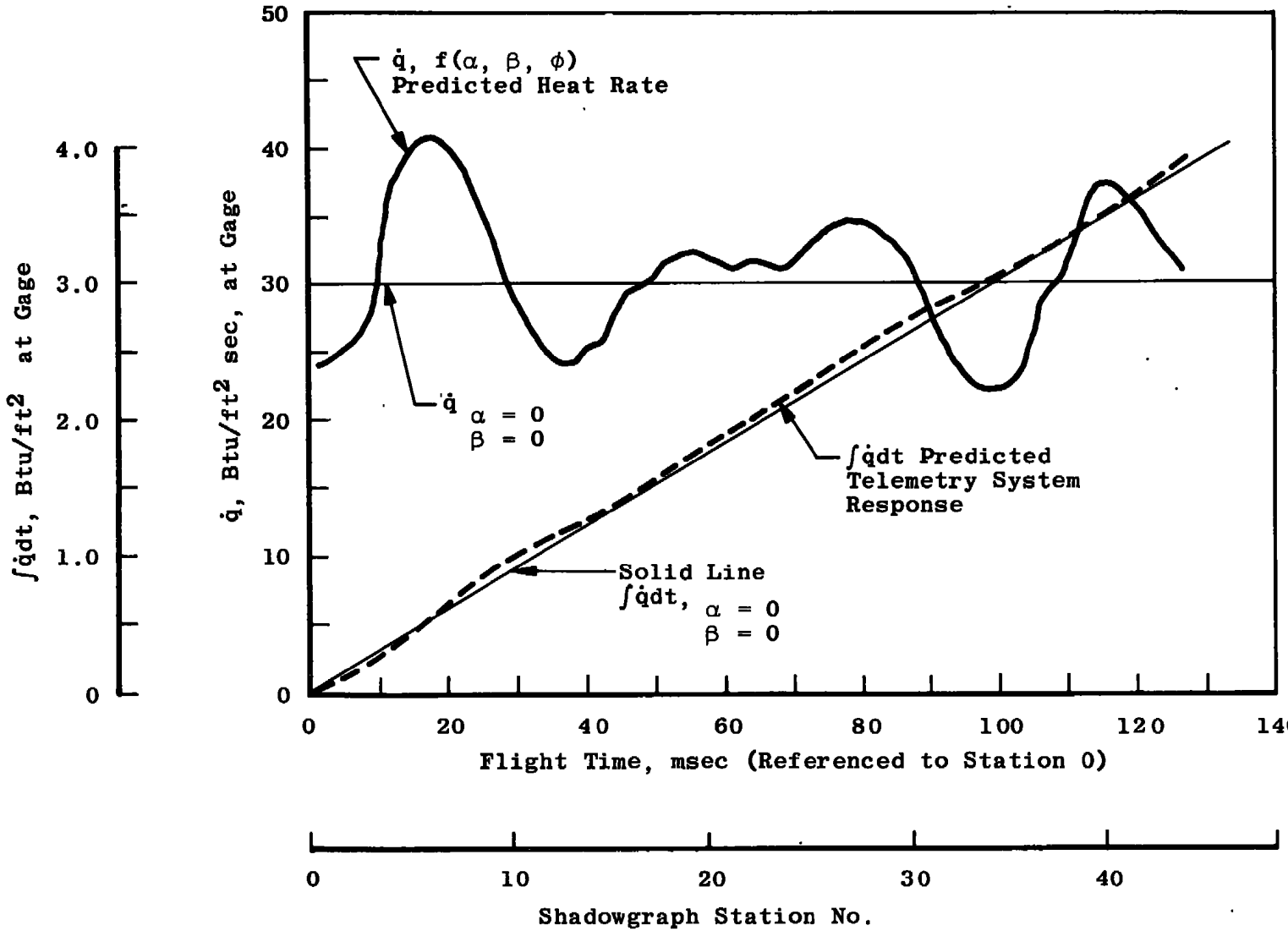

Fig. 20 Shot 2920 Predicted Values

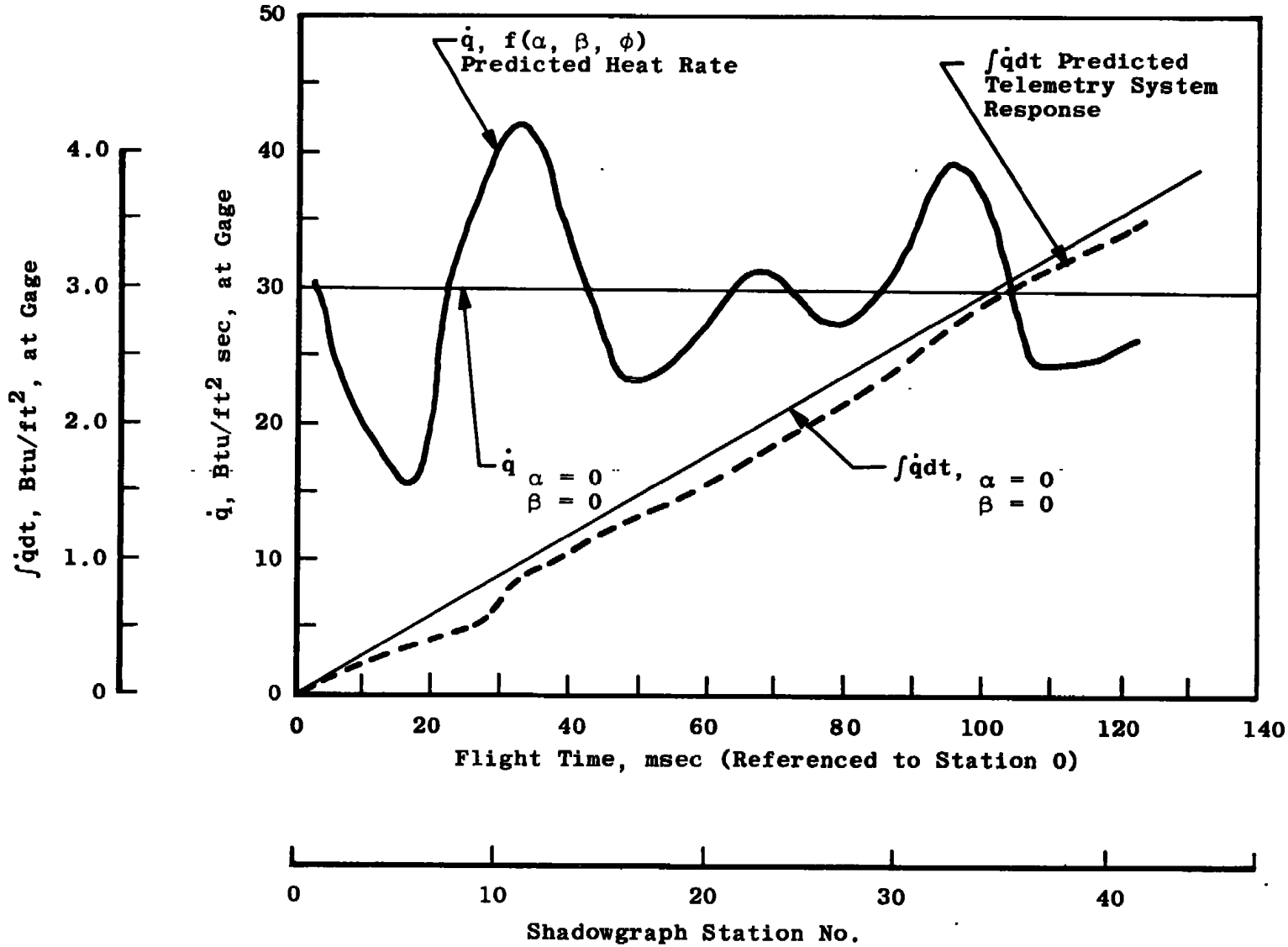

Fig. 21 Shot 2919 Predicted Values

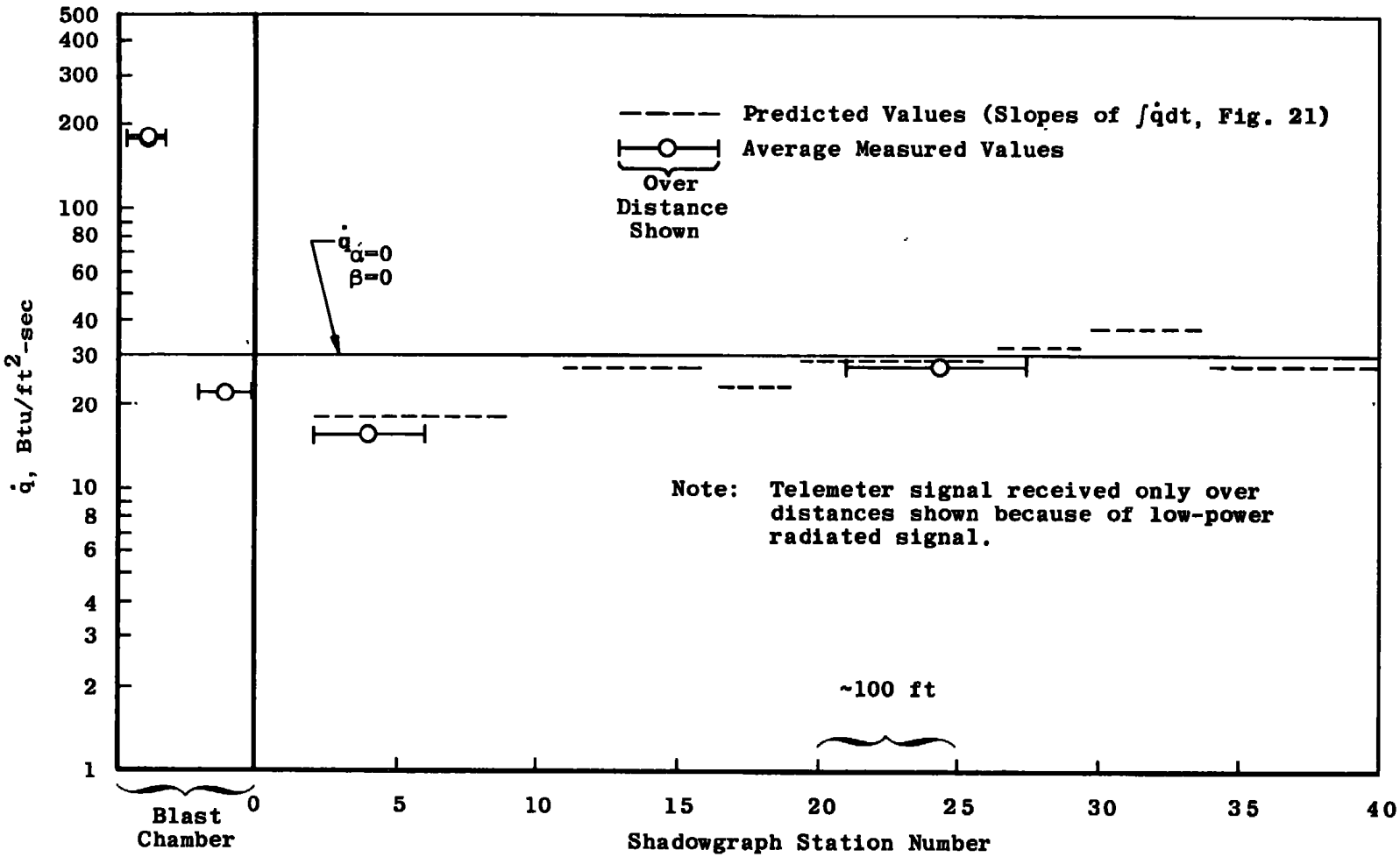

Fig. 22 Comparison of Predicted and Measured Values, Shot 2919

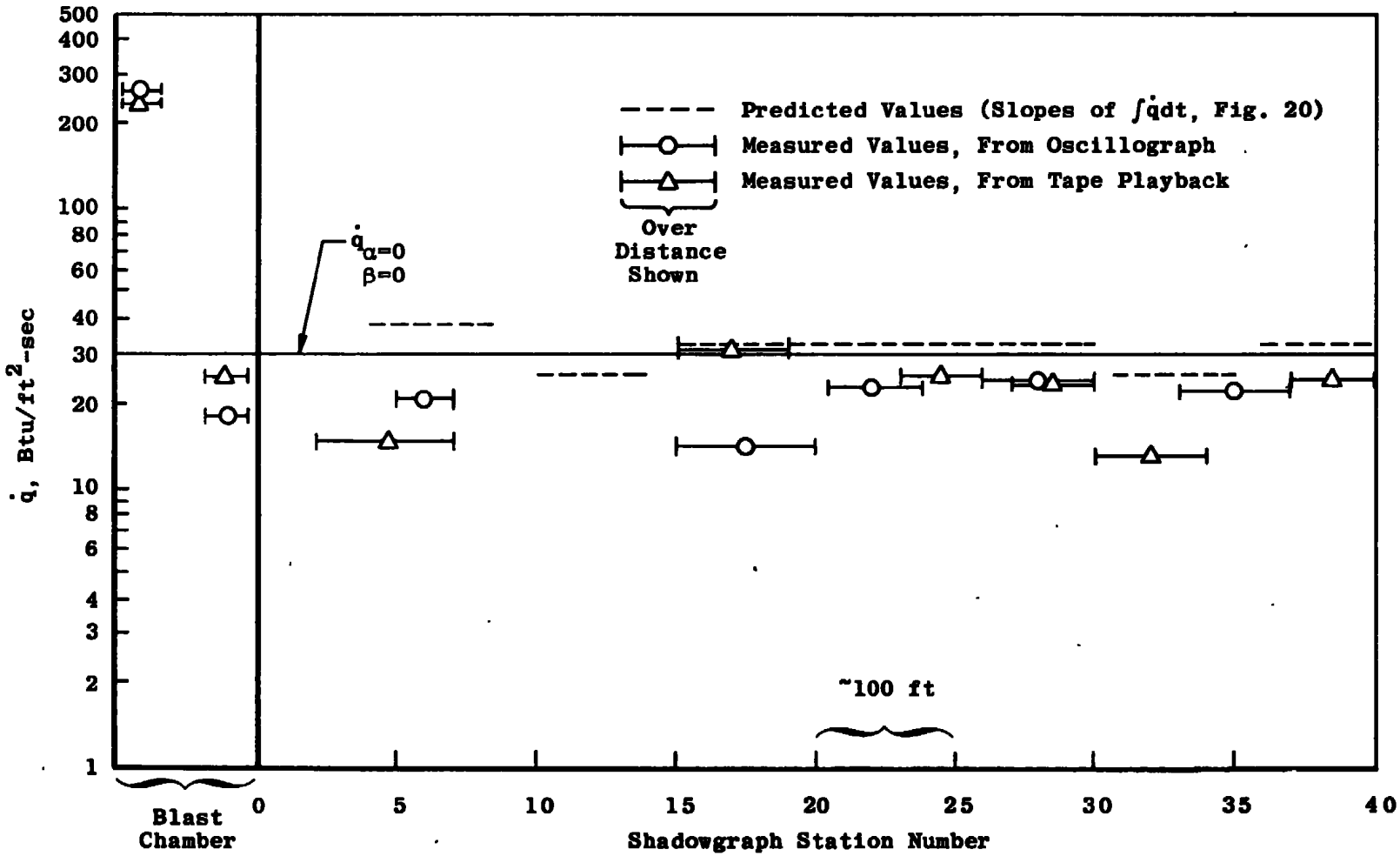

Fig. 23 Comparison of Predicted and Measured Values, Shot 2920

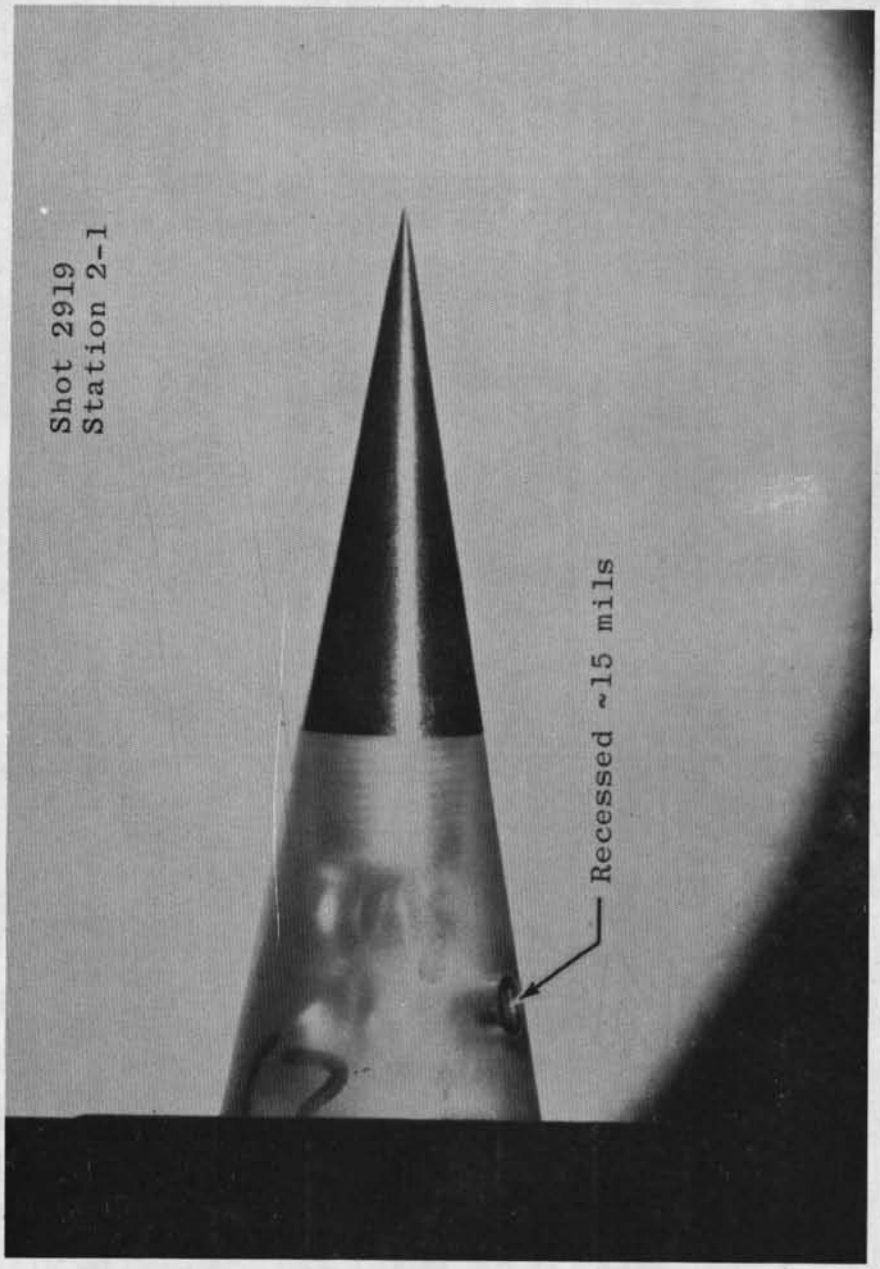

Fig. 24 Gage Recession, Shot 2919

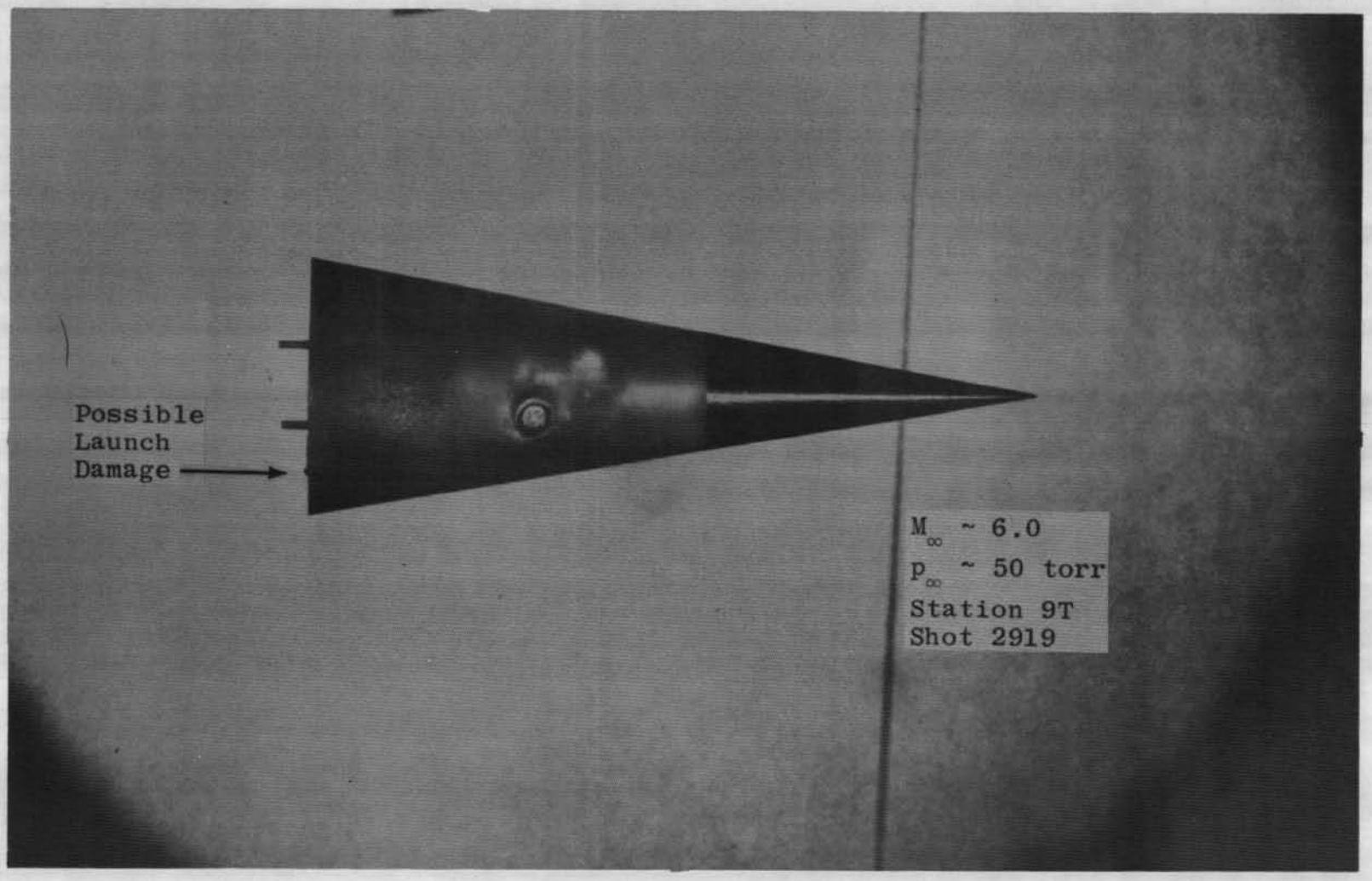

Fig. 25 Shot 2919 Photograph

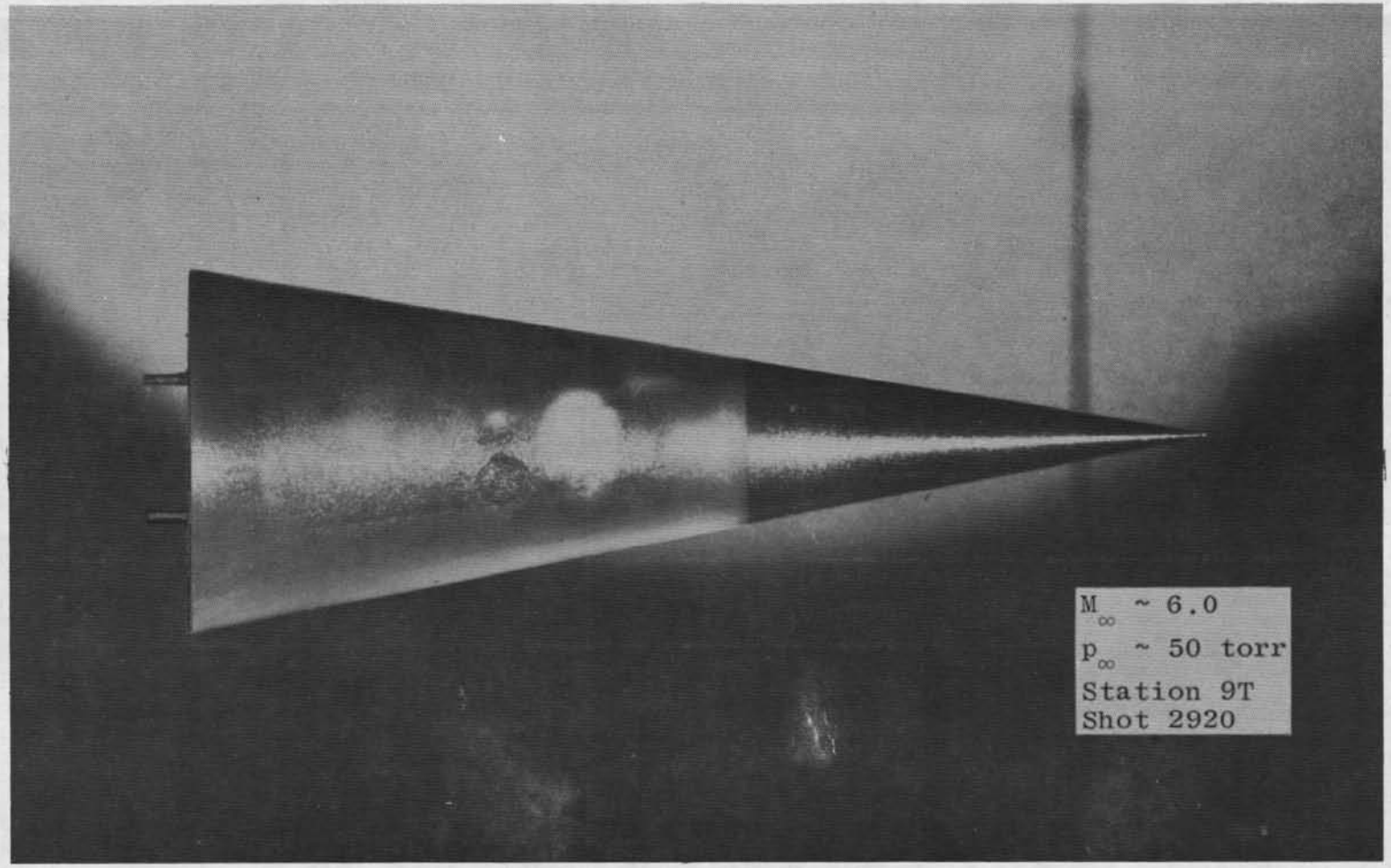

Fig. 26 Shot 2920 Photograph

TABLE I
TYPICAL RECEPTION SYSTEM

Receiver			Antenna Location (See Fig. 9)	Receiver Tuned to:	Monitor Purpose
Channel Number	Bandwidth, MHz	Input,* microvolts			
1	3.3	6	Downrange (Sta. 23)	f_o***	$\dot{q}$ Data
2**	3.3	6	Long Wire	f_o - 8.5 MHz	Gage Open Circuit
3	1.0	4	Downrange	f_o - 2 MHz****	High $\dot{q}$
4	1.2	60	Downrange	f_o + 40 MHz	VVC Open Circuit
5	1.2	60	Uprange	f_o	$\dot{q}$ Data
6	1.2	60	Blast Chamber	f_o	$\dot{q}$ Data

*Minimum input required for satisfactory operation using direct modulation techniques; see text.

**Channel 2 receiver, which monitors open-circuited gage, uses long wire antenna. If gage circuit opens downrange of bulkhead, no signal is received on this channel (see Fig. 9).

***f_o is pre-launch telemeter operating frequency.

****Upper band edge of Receiver 3 tuned to same frequency as lower band edge Receiver 1.

TABLE II
EFFECTS OF CAPACITOR FAILURE ON TRANSMITTER OPERATION

Capacitor Number (See Figure Below)	Effect on Operating Frequency, f_o
1	No RF Output
2	Increases ~60 MHz
3	Increases ~20 MHz
4	Changes 0 ± 2 MHz; See Text
5 (VVC)	Increases ~40 MHz
6	No RF Output*

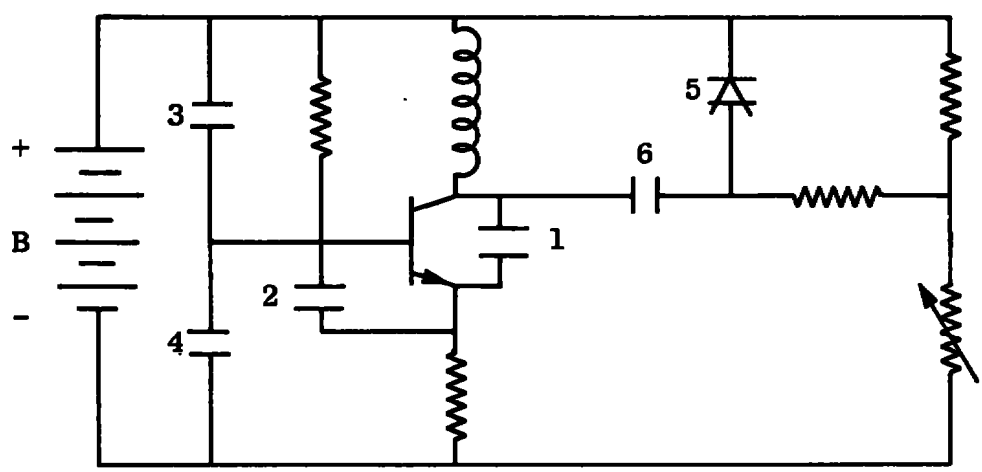

*Transmitter possibly could be operating, but above the upper tuning limit of the receiver (260 MHz).

TABLE III
RESULTS OF STATIC COMPRESSION TESTS

Circuit No:	Operating Frequency, MHz	Frequency Shift after Load Removal, kHz					Comments
		2 klb	4 klb	6 klb	8 klb	10 klb	
7	142	+25	+50	+80	+100	+125	No large frequency jumps recorded.
9	142	+20	-40	+100	+125	+150	Large frequency jumps while loading to 4, 6, and 8 klb.
10	143	+20	+50	+85	+110	+130	No large frequency jumps recorded.
11	196	+10	+25	+50	+60	+140	Large frequency jump while loading to 10 klb.
12	198	+10	+30	+50	+80	+90	Large frequency jumps occurred while loading to 8 and 10 klb.
13	196	+15	+50	+75	+100	+130	Large frequency jump while loading to 8 klb.
DM-2	141	+20	+50	+90	+115	+180	Large frequency jump while loading to 10 klb.
DM-3	140	+20	+60	+100	+120	+140	No large frequency jumps.
DM-4	143	+20	+60	+100	+130	+150	Large frequency jumps while loading to 8 and 10 klb.

TABLE IV
RESULTS OF GUN-RANGE TESTS

Shot No.	Date	Transmitter Type	Purpose of Shot	Notes	Results
2562	11/17/70	Thin Film	Impulse Test; $\dot{q}$ Data	Type A Gage	Large Δf (~ -500 kHz) which fluctuated in accordance with model motion. Possible high, unexpected heat rate in barrel or in flight. Possible circuit malfunction. No $\dot{q}$ data; data slope wrong direction.
2565	11/20/70	Thin Film	Impulse Test	Type A $\dot{q}$ Gage Recessed and Covered with Epoxy	Constant Δf of ~ +600 kHz, with no fluctuation. Possible circuit malfunction. Possible gage loading, causing Δf by permanent deformation. No $\dot{q}$ data possible because of covered gage.
2566	11/23/70	Thin Film	Impulse Test; $\dot{q}$ Data	5-Piece Sabot (See Text) Type A Gage	No output in flight; possible gage failure; possible circuit failure.
2570	11/25/70	Thin Film	Impulse Test	No $\dot{q}$ gage; Replaced with Resistor	No output in flight; concluded circuitry at fault.
2662	1/11/71	Cordwood	Impulse Test; $\dot{q}$ Data*	5-Piece Sabot Type A Gage	Model destroyed during launch.
2663	1/12/71	Cordwood	Impulse Test; $\dot{q}$ Data	Same, Except Metal Model	Δf ~ +260 kHz, no $\dot{q}$ data; data trace fluctuating in accordance with model motion; data slope wrong direction. Off course; impacted shield at midrange.
2810	4/8/71	Cordwood-VVC	$\dot{q}$ Data	Type A Gage	Δf ~ -600 kHz (off oscillograph traces) quit about midrange; suspect preheating of $\dot{q}$ gage during launch; possible $\dot{q}$ gage failure in flight.
2811	4/9/71	Cordwood-VVC	$\dot{q}$ Data	Type A Gage	$\dot{q}$ gage opened.
2812	4/12/71	Cordwood-VVC	$\dot{q}$ Data	Type A Gage	Model failed; $\dot{q}$ gage opened.
2886	6/30/71	Cordwood-VVC	$\dot{q}$ Data	Type B Gage	No output in flight.
2919	9/9/71	Cordwood-VVC	$\dot{q}$ Data	Type B Gage	$\dot{q}$ data obtained, see text.
2920	9/10/71	Cordwood-VVC	$\dot{q}$ Data	Type B Gage	$\dot{q}$ data obtained, see text.

*Also christened new Range G launcher.

APPENDIX III
FM/FM TELEMETRY SYSTEM

GENERAL DESCRIPTION

A single-channel, FM/FM transmitter was developed which used a unijunction transistor (UJT) for the subcarrier oscillator (SCO), and a field-effect transistor (FET) for the transmitter. The system contained no more electronic components than the Colpitts-VVC transmitter, yet had two advantages over the latter. First, the FET-SCO system was relatively insensitive to supply voltage variations. A change of supply voltage of 50 percent (from 8 to 4 volts) would result in a data error near 20 percent on the FM/FM system; whereas, a voltage change of 25 percent (corresponding to the loss of one cell) on the Colpitts-VVC system would result in loss of all data. Second, a multichannel FM/FM system would contain considerably fewer on-board components than a multichannel Colpitts-VVC system. It was pointed out in Ref. 5 that, in an FM/FM system, the data are contained in frequency variations of the SCO; thus, this system does not require as high an incoming RF level for satisfactory data recovery as does a direct modulation system such as the Colpitts-VVC. The FM/FM system requires only the addition of another subcarrier, which would share the same transmitter and receiver, for dual-channel data acquisition. The use of Colpitts-VVC transmitters would require a separate, complete transmitter, as well as a separate receiver, for each channel.

SUBCARRIER OSCILLATOR (SCO)

A unijunction transistor was selected for SCO frequency generation. A programmable UJT, known as an anode-gate thyristor, was found to be quite versatile for this application. It was desired to have the UJT work only as a switch, so that the SCO frequency would be a function of lumped components only (including the gage resistance), and not UJT parameters.

The circuit diagram for the SCO shown in Fig. III-1 was developed, which operates as follows: The gate voltage is established by a resistive divider containing the gage. The timing capacitors charge until the anode voltage exceeds the gate voltage, at which time the thyristor fires, discharging the capacitors. The thyristor then resets, and the cycle starts over. Thus, the output voltage is a pulse train whose repetition rate may be varied by changing either the charging resistor, charging capacitor, or gate voltage.

An SCO frequency between 20 and 30 kHz was selected because, at frequencies above 30 kHz, the waveform became quasi-sinusoidal, possibly indicating an influence from UJT parameters. Availability of large-valued components and UJT design criteria determined the lower frequency limit.

As a result of the 10 k-ohm resistor between gate and ground (Fig. III-1), the SCO will remain on if the gage open circuits; however, the operating frequency will drop to about 10 kHz. The other component values shown in Fig. III-1 were determined experimentally as offering a good compromise between modulation characteristics, voltage stability, current drain, and operating frequency.

FET TRANSMITTER

Use of a Type A (depletion mode) FET allowed construction of a transmitter which was much simpler than the present Colpitts-VVC circuit, as may be seen by comparing Fig. III-1 and Fig. 6. This was possible because a Type A FET is a normally-on device with the gate at dc ground; whereas, a conventional transistor in a similar configuration is normally off, and must be biased on to operate.

The transmitter in Fig. III-1 is a Hartley oscillator in a grounded-drain configuration. Its voltage sensitivity was shown previously in Fig. 12. The transmitter is frequency modulated by injecting the SCO signal at the FET's substrate.

STATIC COMPRESSION TESTS

Two static compression test slugs were constructed containing SCO's (only). A fixed 1000-ohm resistor replaced the gage for these tests, and one 220-pF capacitor was used instead of the two 100-pF capacitors shown in Fig. III-1. (This was before the susceptibility of large-valued capacitors to stress was realized.) The 220-pF capacitor opened during epoxy cure on one specimen. The other specimen operated satisfactorily during the test, exhibiting an SCO frequency change of 1.4 percent of center frequency after removal of a 12,000-lb load.

Two FET-Hartley oscillators (Fig. III-1) were also tested in static compression. Neither failed at loads up to 12,000 lb. Permanent frequency shifts remaining after removal of the 12,000-lb loads were 20 and 90 kHz. These values are comparable to the frequency shifts of Colpitts-VVC transmitters, upon removal of 10,000-lb loads (Table III).

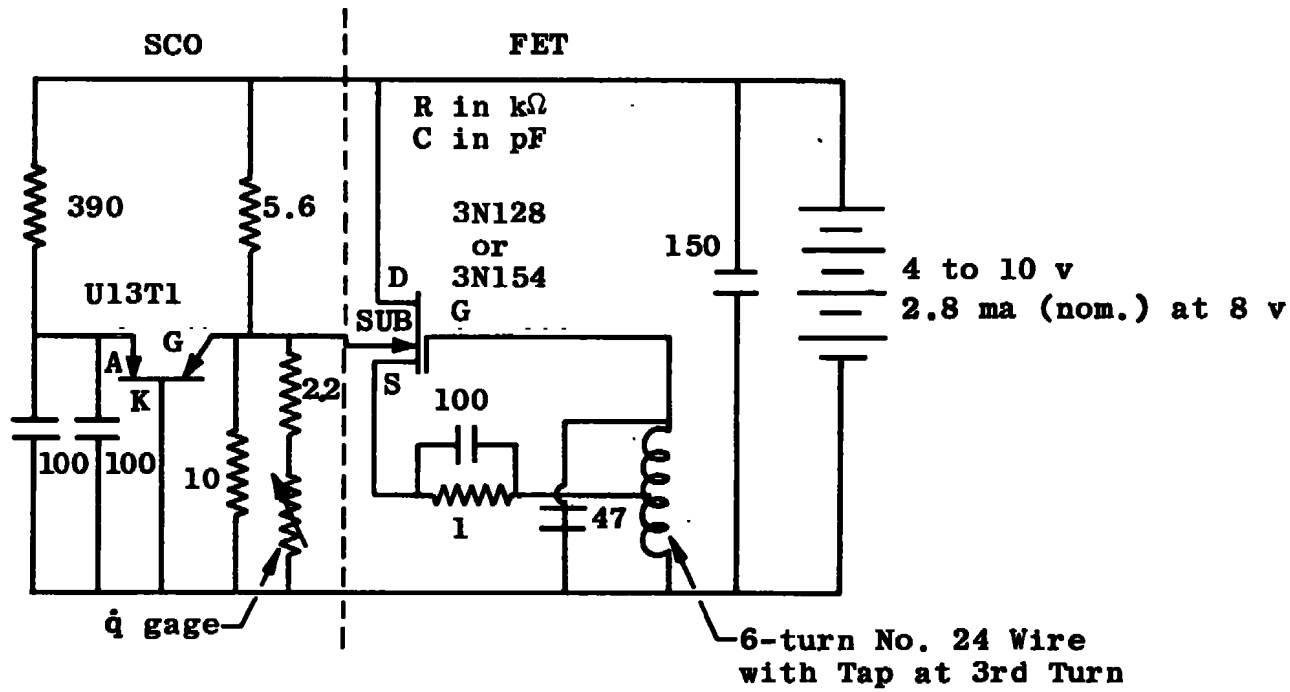

Fig. III-1 SCO-FET System

APPENDIX IV
UNCASED, CERAMIC CAPACITORS

Examination of bench and range test results indicated that a possible cause of the large transmitter shifts observed in Range G, or the failure of a transmitter to operate in flight at all, resulted from failure of one or more of the six glass capacitors used. Unlike transducer failure, capacitor failure is difficult to identify positively. Failure of a capacitor will cause the transmitter to indicate either a large zero shift or will cause the transmitter to shut down completely, as described earlier in Table II. Static compression tests showed that the glass capacitors used invariably failed under load before any of the other components.

Since the glass capacitors had withstood compressive loads during bench tests which were far in excess of the compressive loads expected during launch, another failure mode was felt likely. The effects of shock propagation and tensile loading of the components were strongly suspected. In addition, the glass capacitors are so large that they occupy a sizable portion of the space allotted to the telemetry circuitry aboard the model, which might tend to increase stress concentrations. For these reasons, a search for smaller, more rugged capacitors was begun. Samples of uncased, ceramic capacitors, in the values required, were evaluated. The smaller volume which they would occupy is illustrated by comparing their dimensions with those of the currently used capacitor.

Currently Used Capacitor	360 x 165 x 100	(mils)
Ceramic Type 1	50 x 40 x 40	(mils)
Ceramic Type 2	75 x 50 x 40	(mils)

Thus, by simply changing to ceramic capacitors, the capacitors would occupy less than 0.5 percent of the volume available in the cone model, instead of the 15 percent currently required by the glass capacitors.

To evaluate the ceramic capacitors (relative to glass capacitors), six static compression test slugs containing transmitters were fabricated, two each with the three different types of capacitors. Figure IV-1 is a comparison of the results, and shows no great spread in permanent frequency shifts remaining after load removal, up until 10-kilopound loads were reached. A large, permanent, frequency jump occurred as a 10-kilopound load was being removed from the first SCT slug containing glass capacitors. When an attempt was made to apply a 12-kilopound load, the transmitter appeared to cease operating when 8 kilopounds was reached. By leaving the load applied to the SCT slug,

the receiver was tuned to determine what had failed. It was found that the 150-pF RF bypass between oscillator base and B- had opened. During tests of the second SCT slug containing glass capacitors, a frequency jump of +50 kHz occurred at 9.8 kilopounds on the way to 10-kilopounds load. While loading to 12 kilopounds, the frequency jumped +160 kHz at 6.7 kilopounds. This slug was then cycled between 0 and 12 kilopounds. After six cycles, the transmitter appeared to cease operating at less than 2-kilopound load. Returning the receiver verified that the 150-pF RF bypass between base and B- had again failed. By way of comparison, no discrepancies of any sort appeared during tests of the four remaining SCT slugs containing ceramic capacitors.

The above tests pointed out that there could be a connection between glass capacitor failures and the large, unexplained, transmitter frequency shifts observed during range flight. First, larger-valued glass capacitors consistently failed before smaller-valued ones. Second, capacitors performing the same functions failed in both the above SCT slugs, namely, the "bottom" RF bypass (Fig. 6); yet the "top" RF bypass is of the same value. The same component orientation jig was used to build the SCT slugs as was used to build the range test models. It is possible that it is merely coincidental that the same capacitor failed on both SCT slugs, but it is also possible that use of this particular orientation jig aggravates an already marginal component by positioning it in an area subjected to abnormal stresses.

It should be pointed out that a repeatable, +2 MHz shift was observed when the glass capacitor mentioned above was electrically opened during SCT slug construction. Such was not the case, however, when the same component was opened in a telemetry package contained in a cone model, as described previously; unpredictable frequency shifts in the range from -2 MHz to +2 MHz were observed. Thus, it will be extremely difficult to pinpoint failure of this particular component during flight of a telemetry-equipped cone model in Range G.

In summary, uncased ceramic capacitors were compared with the currently used capacitors by means of static compression test results, and clearly appear to be superior for gun range telemetry purposes.

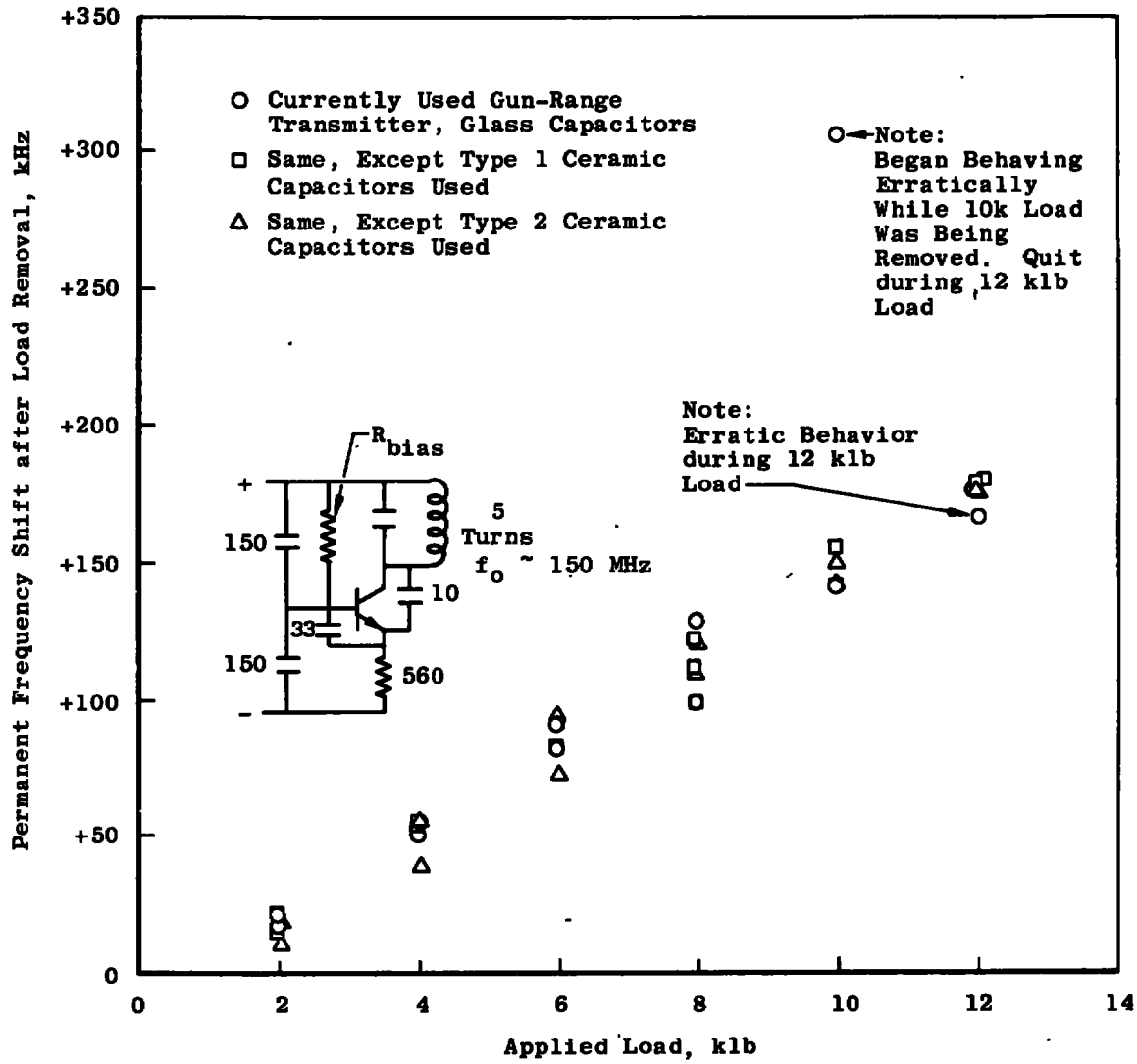

Fig. IV-1 Effects of Static Load

UNCLASSIFIED

Security Classification

DOCUMENT CONTROL DATA - R & D

(Security classification of title, body of abstract and indexing annotation must be entered when the overall report is classified)

1 ORIGINATING ACTIVITY *(Corporate author)* Arnold Engineering Development Center, Arnold Air Force Station, Tennessee 37389.	2a. REPORT SECURITY CLASSIFICATION UNCLASSIFIED 2b. GROUP N/A

3. REPORT TITLE

RADIO TELEMETRY DEVELOPMENT FOR AEROBALLISTIC RANGE TESTS

4 DESCRIPTIVE NOTES *(Type of report and inclusive dates)*

July 1, 1970, to September 10,1971--Summary Report

5. AUTHOR(S) *(First name, middle initial, last name)*

R. H. Choate, ARO, Inc.

6. REPORT DATE	7a. TOTAL NO. OF PAGES	7b. NO. OF REFS
April 1972	72	11

8a. CONTRACT OR GRANT NO.	9a. ORIGINATOR'S REPORT NUMBER(S)
Program Element 64719F	AEDC-TR-72-37
	9b. OTHER REPORT NO(S) *(Any other numbers that may be assigned this report)* ARO-VKF-TR-72-8

10. DISTRIBUTION STATEMENT Distribution limited to U. S. Government agencies only; this report contains evaluation of commercial equipment; April 1972; other requests for this document must be referred to Arnold Engineering Development Center (XON), AFSC, Arnold AF Stn., Tennessee 37389.

11. SUPPLEMENTARY NOTES	12. SPONSORING MILITARY ACTIVITY
Available in DDC	Arnold Engineering Development Center (XON), Arnold Air Force Station, Tennessee 37389.

13. ABSTRACT

An aeroballistic range telemetry system, developed for heat-transfer measurements, was evaluated by means of static and dynamic tests and then subjected to actual range launchings. Heat-transfer information was telemetered from conical models in flight on two successive launches in the VKF 1000-ft Hyperballistic Range (G). The models, sharp, 10-deg (half-angle) cones of 2.0-in. base diameter, were in free flight near Mach 6 at free-stream pressures near 50 torr. Heat-transfer transducers were located on the conical surfaces at 69.4 percent of the distance from the nose to the base. Telemetered heat-transfer rates, in the vicinity of 25 Btu/ft^2-sec, were about 10 and 25 percent below theoretically predicted values on these two shots. Several possible reasons for disagreement between telemetered and theoretical data are identifiable.

DD FORM 1 NOV 65 1473

UNCLASSIFIED

Security Classification

14. KEY WORDS	LINK A		LINK B		LINK C	
	ROLE	WT	ROLE	WT	ROLE	WT
radio telemetry						
data transmission						
aeroballistic ranges						
test facilities						
scale model						
aerodynamic characteristics						

AFSC
Arnold AFS Tenn